9
Joining of Composite Structures

9.1 Introduction

Airframe structures consist essentially of an assembly of simple elements connected to form a load transmission path. The elements, which include skins, stiffeners, frames, and spars, form the major components such as wings, fuselage, and empennage. The connections or joints are potentially the weakest points in the airframe so can determine its structural efficiency.

In general, it is desirable to reduce the number and complexity of joints to minimize weight and cost. A very important advantage of composite construction is the ability to form unitized components, thus minimizing the number of joints required. However, the design and manufacture of the remaining joints is still a major challenge to produce safe, cost-effective, and efficient structures.

This chapter is concerned with joints used to connect structural elements made of advanced fiber composite laminates, mainly carbon/epoxy (carbon/epoxy), to other composite parts or to metals. Sections 9.3 and 9.4 deal, respectively, with bonded and mechanical joints typical of those used in the manufacture of airframe components. Joints are also required to repair structural damage; this topic is dealt with in Chapter 10. Both design and materials aspects are considered. The aim of this chapter, when discussing design, is to outline simple analytical procedures that provide a physical insight into the behavior of joints involving composites. The materials aspects covered will be those essential to the manufacture of sound joints.

Joint types used in airframe construction can be broadly divided into joints that are mechanically fastened using bolts or rivets, adhesively bonded using a polymeric adhesive, or that feature a combination of mechanical fastening and adhesive bonding.

In mechanical joints, loads are transferred between the joint elements by compression on the internal faces of the fastener holes with a smaller component of shear on the outer faces of the elements due to friction. In bonded joints, the loads are transferred mainly by shear on the surfaces of the elements. In both cases, the load transmission elements (fastener or adhesive) are stressed primarily in shear along the joint line; however, the actual stress distribution will be complex.

Joints can be classified as single or multiple load path. Single load path joints are joints in which failure would result in catastrophic loss of structural capability. Multiple load path joints are joints in which failure of a single element results in the load being carried by other load-carrying members. An apparently multiple load path joint would be classified as single load path if failure of one of the paths leads to an unacceptable reduction in the load capacity of the joint.

The alignment of the load path and the geometry of the structural elements are important considerations in the design of joints. Airframe structural elements are usually intended to be loaded in either tension/compression or shear. Primary bending is avoided by keeping the loading as close as possible to collinear. However, secondary bending induced by minor eccentricity of the loads occurs in many types of joint (and structure) and can cause serious problems.

Compared with metals, laminated fiber composites have relatively low through-thickness strength and bearing strength under concentrated loads. Thus metals, usually titanium alloys, are sometimes required to transmit loads in and out of highly loaded composite structure, particularly where stress fields are complex.

Typical design parameters for carbon/epoxy airframe components (for a high-performance military aircraft) are:

- Ultimate design strain: $\pm$ 3000 to 4000 microstrain for mechanically fastened structure, up to $\pm$ 5000 microstrain for bonded honeycomb structure
- Operating temperature -55 °C to $+105$ °C
- Service fluids; presence of moisture, hydraulic oil, fuel, and (limited exposure to) paint stripper

Strain, rather than strength, is generally used as the basis for comparison of the structural capacity of composite structure because composites of differing stiffness tend to fail at a similar strain level—particularly when damaged. Microstrain is strain $\times 10^{-6}$.

9.2 Comparison Between Mechanically Fastened and Adhesively Bonded Joints

The advantages and disadvantages of forming joints by adhesive bonding and bolting or riveting are summarized in Table 9.1

Although there are many advantages for bonding composites from the performance view point, there are also many limitations or disadvantages that must be considered with each potential application. For a relatively thin-skinned structure, particularly where fatigue may be a problem, bonding is very attractive indeed. However, the use of suitable pre-bonding surface treatments and adhesives is essential to develop the required strength level and maintain it during a service life, which could be more than 30 years.

A high level of quality control is very important to obtain reliable adhesive bonding. This is because current non-destructive inspection (NDI) procedures are able to detect only gross defects such as severe voids and disbonds in bonded

Table 9.1 A Comparison of the Advantages and Disadvantages of Adhesively Bonded and Bolted Composite Joints

Advantages	Disadvantages
Bonded Joints	
Small stress concentration in adherends	Limits to thickness that can be joined with simple joint configuration
Stiff connection	Inspection other than for gross flaws difficult
Excellent fatigue properties	Prone to environmental degradation
No fretting problems	Sensitive to peel and through-thickness stresses
Sealed against corrosion	Residual stress problems when joining to metals
Smooth surface contour	Cannot be disassembled
Relatively lightweight	May require costly tooling and facilities
Damage tolerant	Requires high degree of quality control
	May be of environmental concern
Bolted Joints	
Positive connection, low initial risk	Considerable stress concentration
Can be disassembled	Prone to fatigue cracking in metallic component
No thickness limitations	Hole formation can damage composite
Simple joint configuration	Composites's relatively poor bearing properties
Simple manufacturing process	Pone to fretting in metal
Simple inspection procedure	Prone to corrosion in metal
Not environmentaly sensitive	May require extensive shimming
Provides through-thickness reinforcement; not sensitive to peel stresses	
No major residual stress problem	

components but are unable to detect weak or (due to environmental degradation) potentially weak bonds. The limitations of NDI are a major reason why adhesive bonding has rarely been used in critical primary joints in metallic airframe structure; bonded metal joints are particularly prone to environmental degradation if not adequately surface-treated.

Mechanical fastening is usually the lower-cost option because of its simplicity and low-cost tooling and inspection requirements. However, hole-drilling can be highly labor intensive (unless automated) and, if not correctly done, can be highly damaging to the composite. Joints in aircraft usually require many thousands of expensive fasteners (usually titanium alloy), and extensive shimming may be required to avoid damage to the composite structure during bolt clamp-up. Thus adhesive bonding, despite the high tooling, process, and quality control costs, can in many cases offer significant cost savings.

9.3 Adhesively Bonded Joints

Symbols

Shear modulus (also used for strain energy release rate)	G	Young's modulus	E
Shear stress	τ	Stress	σ
Shear strain	γ	Strain	ε
Thickness	t	Displacement	U
Transfer length	L		
Plastic zone size	d	Applied load	P
Step length	N	Transmitted load	T
Scarf angle	θ	Thermal expansion coefficient	α
		Temperature range	ΔT

$\Delta T =$ (service temperature—cure temperature)

Subscripts/Superscripts

Plastic condition	p	Outer adherend (also for mode 1 opening)	1
Elastic condition	e	Inner adherend (also for mode 2 opening)	2
Ultimate value	u	Maximum value	max
Adhesive	A	Minimum value	min
Temperature	T	Balanced	b
Value at infinite length	∞	Unbalanced	un
Critical value	C		

9.3.1 Introduction

Bonded joints used in aerospace applications can be classified as single (primary) or multiple (secondary) load path joints, as indicated in Figure 9.1. This section describes simple design procedures and some materials' engineering aspects relevant to the application of these types of joint in airframe structures.

In the design of bonded composite joints, consideration is given to each of the elements to be joined (adherends), including their geometry, size, materials of construction, actual or potential modes of failure, coefficients of thermal expansion, magnitude and nature of the loading involved, and operating environment.

Potential modes of failure are:

- Tensile, compressive, or shear of the adherends
- Shear or peel in the adhesive layer
- Shear or peel in the composite near-surface plies
- Shear or peel in the resin-rich layer on the surface of the composite
- Adhesive failure at the metal or composite/adhesive interface

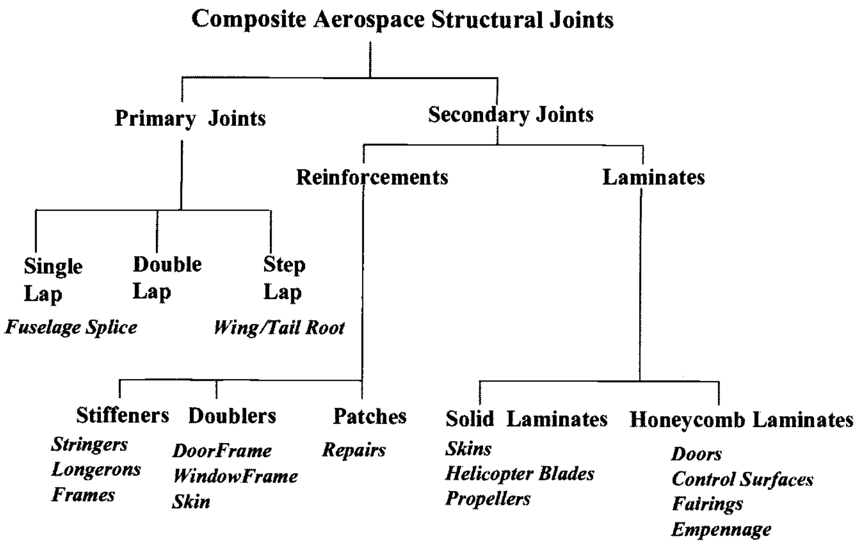

Fig. 9.1 Classification and applications of adhesively bonded joints used in airframe manufacture.

The design aim is for the joint to fail by bulk failure of the adherends. A margin of safety is generally included in the design to provide tolerance to service damage and manufacturing defects in the bond line. Generally, the adhesive is not allowed to be or to become the weak link[1] because adhesive strength can be highly variable, and the growth of damage or defects in the adhesive layer can be very rapid under cyclic loading. For composite adherends, the very thin, relatively brittle resin bonding the near-surface plies is more prone to failure than the adhesive layer, so great care must also be taken to ensure that this does not become the weak link.

The design input parameters include:

- Stiffness and strength (for metals usually the yield strength) of the adherends
- Shear modulus, yield strength, and strain-to-failure of the adhesive
- Thermal expansion coefficient of the adherends
- Magnitude and direction of the applied loads
- Overlap length of the adherends
- Thickness of the adherends
- Thickness of the adhesive

The properties used must be sufficient to handle the weakest state of the materials; for the adhesive and composite adherends, this is usually the hot/wet condition. It is most important to ensure that the strength of the adherend/adhesive interface does not become significantly weakened as a result of environmental degradation. For a degraded interface, there is no way of quantifying minimum strength; even zero is a possibility. Environmental degradation of the interface in service is much more likely if the adherends are not given the correct surface treatment before bonding. Suitable methods will be discussed later.

Fatigue damage or creep in the adhesive layer can be avoided, or at least minimized, by maintaining the adhesive in an elastic state for most of its service life. Ideally, significant plastic deformation of the adhesive should be permitted only when the joint is stressed to limit load. Limit load is the highest load expected during the service life of the aircraft. Even at ultimate load (1.5× limit), the strain in the adhesive should not approach the failure strain.

The design aim is to maintain the adhesive in a state of shear or compression. Structural adhesive joints (and composites) have relatively poor resistance to through-thickness (peel) stresses and, where possible, this type of loading is avoided. The classical joint types, suitable for joining composites to either composites or metals[2] (Fig. 9.2), are 1) the double lap, 2) the single lap, 3) the single scarf, 4) double scarf, 5) the single-step lap, and 6) the double-step lap.

Figure 9.3, by Hart-Smith,[3] illustrates schematically the load-carrying capacities of these joints and some simple design improvements.

The single-lap joint is generally the cheapest of all joints to manufacture. However, because the loads are offset (eccentric), a large secondary bending moment develops that results in the adhesive being subjected to severe peel stresses. This type of joint is therefore only used for lightly loaded structure or is supported by underlying structure such as an internal frame or stiffener.

The double-lap joint has no primary bending moment because the resultant load is collinear. However, peel stresses arise due to the moment produced by the unbalanced shear stresses acting at the ends of the outer adherends. The resulting stresses, although relatively much smaller in magnitude than in the single-lap joint, produce peel stresses limiting the thickness of material that can be joined. Peel (and shear) stresses in this region are reduced by tapering the ends of the joint. As shown in Figure 9.3, this markedly increases the load capacity of this joint.

The scarf and step-lap joints, when correctly designed, develop negligible peel stresses and may be used (at least in principle) to join composite components of any thickness.

To explore the feasibility of using primary lap joints that use only adhesive bonding, the USAF funded the Primary Adhesively Bonded Structure Technology (PABST) program[4] which, although concerned with the bonding of aluminum alloy airframe components, must be mentioned as a landmark in the development of bonded joints for aeronautical applications; many of its conclusions are relevant to bonded composite construction. The Douglas Aircraft Company was the major contractor. The program (based on a full-scale section of fuselage for a military transport aircraft) demonstrated that significant improvements could be obtained in integrity, durability, weight, and cost in an

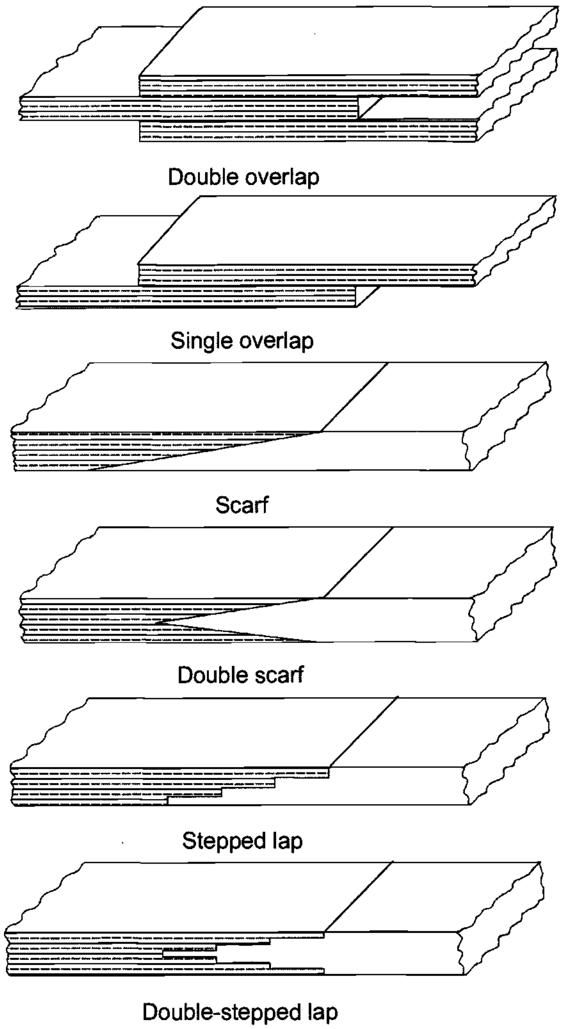

Fig. 9.2 Schematic illustration of several types of bonded joint.

aluminum alloy fuselage component by the extensive use of bonded construction. The demonstrated weight-saving was about 15%, with a 20% saving in cost.

Lap joints relying solely on adhesive bonding, although structurally very attractive, are not generally used by major aircraft manufacturers in primary structural applications (such as fuselage splice joints) because of concerns with long-term environmental durability. These concerns stem from some early poor service experience with the environmental durability of adhesive bonds, resulting from the use of inadequate pre-bonding surface treatments and ambient-curing adhesives.

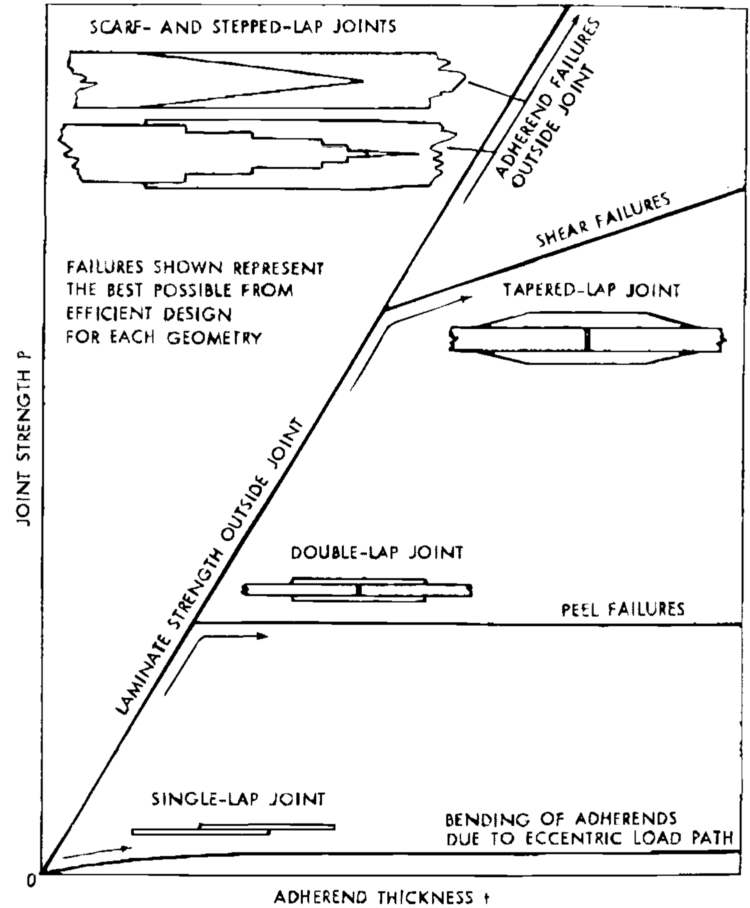

Fig. 9.3 Load-carrying capacity of adhesive joints. Taken from Ref. 3.

9.3.2 Design/Analysis of Bonded Lap Joints

Reviews of analytical procedures for joints involving composites are provided in Refs. 5 and 6. Hart-Smith undertook comprehensive analytical studies[7–9] on adhesive joints, particularly advanced fiber composite to composite and composite to metal joints. His studies, based on the earlier approaches, cover the important aspect of non-linear (elastic/plastic) deformation in the adhesive. The stress level for joint (adhesive) failure is determined by shear strain to failure of the adhesive ($\gamma_e + \gamma_p$) in the bondline; the design aim being that this stress level should well exceed adherend strength. Peel stresses are avoided by careful design rather than considered as a potential failure mode.

Several earlier attempts were made to represent non-linear behavior in the adhesive assuming realistic shear stress/shear strain behavior, but they were too

Table 9.2 Computer Programs Developed by Dr John Hart-Smith for Stress Analysis of Bonded Joints

Joint to be analyzed	Program	Joint to be analyzed	Program
Single-lap joint: Joint strengths and efficiencies in non-dimensional form. *Deals only with identical adherends. Three failure cases are considered: a) adherend bending, b) adhesive shear, and c) adhesive peel.*	A4EA	Double-lap joint: Elastic adherend and elastic/plastic adhesive. *Can deal with unbalanced joints and allows for thermal mismatch between adherends. Provides ratio of maximum to average shear strength and non-dimensionalized joint strength.*	A4EB
Scarf Joint: Elastic adherend and elastic/plastic adhesive. *Provides a) shear stress distribution along the joint b) displacement of inner and outer adherends, and c) potential joint strength.*	A4EE	Step-lap joint: Elastic adherend and elastic/plastic adhesive. *Provides a) shear stress distribution along the joint, b) displacement of inner and outer adherends, and c) potential joint strength.*	A4EG
Step-lap joint: Elastic adherend and elastic/plastic adhesive. *Similar to A4EG but more comprehensive; allows for variations in adhesive thickness and adhesive defects. Bond width can also be varied.*	A4EI		

complex for most analytical approaches. However, as discussed later, Hart-Smith shows that a simple elastic/ideally plastic formulation gives similar results to more realistic representations of adhesive behavior, providing the strain energy density in shear in the adhesive (area under the stress-strain curve) is comparable to that expected for the real curve.

As a major part of these studies, software programs were developed for the analysis of double-overlap and the other types of joint discussed here; these are listed in Table 9.2. Similar programs are available through the Engineering Sciences Data Unit (ESDU)$_9$ and proprietary programs have been developed by manufacturers.

Inevitably, many of the complications in real joints are neglected or inadequately dealt with in these relatively simple studies. These include:

- Influence of flaws in the form of local porosity, local disbonds, etc.
- Adhesive thickness variations
- Through-thickness variation of shear stresses
- Through-thickness stresses
- Stress-free state at the ends of the adhesive
- Highly beneficial effect of adhesive spew, excess adhesive that forms a fillet at the edges of the joint
- True shear stress/shear strain behavior

Most of these complexities are best modelled using finite element procedures. For example, the simple analytical procedures for lap joints mentioned here predict that the maximum shear stress occurs at the free ends of the overlap. However, because the end of the overlap is a free surface, the principle of complimentary shears is violated because the horizontal shear force at the ends cannot be balanced by a vertical shear force. In reality, therefore, the stress along the bond line right at the edge must fall to zero. More realistic stress analysis—using the finite element approach[10] shows that this is the case—shear stress falls rapidly to zero over a distance of the order of the adherend thickness; these observations are confirmed by direct experimental observations. However, the shear stress distribution along the bond line and magnitude of the maximum stress predicted by the simple analytical procedures turns out to be approximately correct. Similar observations have been made concerning normal or peel stresses.

A further considerable complication, difficult to handle even with finite element methods, is the time dependency or viscoelastic (and viscoplastic) behavior of adhesives.

9.3.3 Models for Adhesive Stress/Strain Behavior

For analysis of stress distribution in the joint, a model for the shear stress/strain behavior of the adhesive is required. The simplest model assumes that the adhesive is strained only within its linear elastic range. This model may be adequate if fatigue is a major concern and the primary aim is to avoid plastic cycling of the adhesive; then the stresses must not be allowed to exceed τ_p. However, use of the elastic model is overly conservative for assessing the static strength of a joint, particularly if it is bonded with a highly ductile adhesive.

To account for plastic deformation, the actual stress/strain behavior must be modelled. In computer-based approaches such as the finite element method, the stress/strain curve can be closely modelled using the actual constitutive relationship. However, for analytical approaches, much simpler models are needed.

Figure 9.4 shows stress/strain behavior for a typical ductile adhesive and the models of this behavior used for joint analysis by Hart-Smith.[11] The intuitive simple non-linear model is the bilinear characteristic because this most closely approximates to the real curve. However, even use of this simple model is mathematically complex, greatly limiting the cases that can be analyzed to produce closed-form solutions.

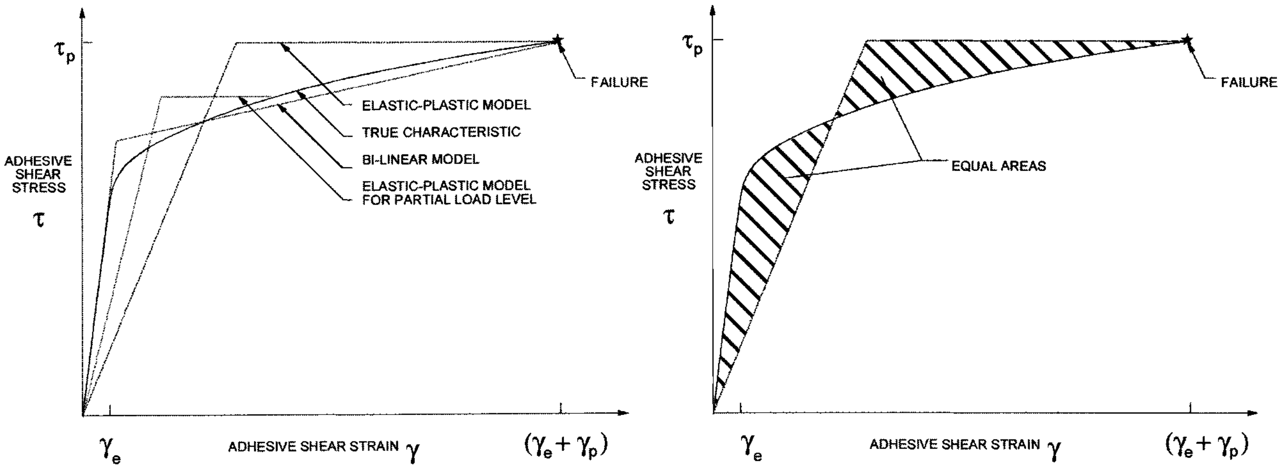

Fig. 9.4 Models for representing the shear stress/strain behavior in an adhesive. Taken from Ref. 11.

The ideally elastic/plastic models, (Fig. 9.4), greatly simplify the analysis, allowing closed-form solutions to be developed for a wide range of joints. It is shown that the requirement for the elastic/ideally plastic model is that it has the same shear strain energy (area under the curve) as the actual curve and intersects it at the required level of shear stress. Thus, as indicated in Figure 9.4, the effective shear modulus G_A and shear yield stress used in the model vary with the strain level.

In most joint designs, it is sufficient to undertake a simple elastic analysis to check that, for most of the operation of the joint (below limit load), the adhesive will not deform plastically and then, using the effective elastic/plastic parameters, assess the load-carrying capacity of the joint.

For the strength analysis to be conservative, the hot/wet shear yield strength should be used to assess the likelihood of fatigue damage, then the low-temperature stress/strain behavior of the adhesive used to estimate static strength (because the area under the stress–strain curve is then a minimum).

9.3.4 Load Transfer Mechanisms in Overlap Joints

The skin/doubler joint shown in Figure 9.5 provides a simple illustration of the main features of load transfer in a lap joint. The overlap length is assumed to be semi-infinite, which means that it is very much larger than the load-transfer length based on the exponent β.

Loading of the outer adherend occurs by the development of surface shear forces, which arise as the adhesive layer resists the shear displacement between the inner, directly loaded adherend and the outer, initially unloaded, adherend. Load transfer by the shear forces produces an increasing axial strain in the outer (reinforcing) adherend and a reducing strain in the inner adherend until, at some point, the strains in the two adherends become equal; the shear strain in the adhesive is then zero.

9.3.4.1 Elastic Model for the Adhesive. The analysis assuming elastic behavior is outlined in Figure 9.5, and the outcome is illustrated in Figure 9.6. It is assumed here that failure occurs when $\tau_{\max} = \tau_p$ for the adhesive. Bending effects, for example, due to joint rotation, are not considered in this analysis. It therefore corresponds to a symmetric double-lap joint or symmetric doubler configuration, or a single-lap/single-sided doubler configuration in which bending is reacted by other supporting structure.

The main analytical results from this model are as follows:

Shear stress and strain distributions are given by:

$$\tau = \tau_P e^{-\beta x} \tag{9.1}$$

$$\gamma = \gamma_P e^{-\beta x} \tag{9.2}$$

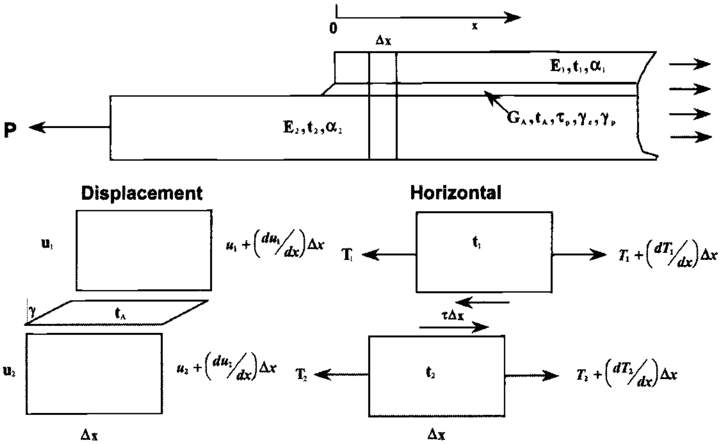

Equilibrium: $\dfrac{dT_1}{dx} - \tau = 0$

$\dfrac{dT_2}{dx} + \tau = 0$

Material: $\tau = G_A \gamma$

$\sigma = E\varepsilon \Rightarrow \dfrac{T_1}{t_1} = E_1 \dfrac{du_1}{dx}$

$\dfrac{T_2}{t_2} = E_2 \dfrac{du_2}{dx}$

Compatibility: $\gamma = \dfrac{u_1 - u_2}{t_A}$

$$\therefore \tau = G_A \frac{u_1 - u_2}{t_A} \quad \textit{and} \quad \frac{d\tau}{dx} = \frac{G_A}{t_A}\left(\frac{du_1}{dx} - \frac{du_2}{dx}\right)$$

$$\therefore \frac{d\tau}{dx} = \frac{G_A}{t_A}\left(\frac{T_1}{E_1 t_1} - \frac{T_2}{E_2 t_2}\right)$$

$$\therefore \frac{d^2\tau}{dx^2} = \frac{G_A}{t_A}\left(\frac{1}{E_1 t_1} + \frac{1}{E_2 t_2}\right)\tau$$

$$\therefore \tau = \tau_{x=0} e^{-\beta x} \quad \textit{where} \quad \beta^2 = \frac{G_A}{t_A}\left(\frac{1}{E_1 t_1} + \frac{1}{E_2 t_2}\right)$$

Fig. 9.5 Configuration and analysis of a single-lap joint.

where

$$\beta^2 = \frac{G_A}{t_A}\left[\frac{1}{E_1 t_1} + \frac{1}{E_2 t_2}\right] \tag{9.3}$$

Because of the low shear moduli of polymer-matrix composites, a modification[12] of this equation is required to estimate β. This can be done (assuming a linear shear lag across the thickness) by replacing t_A/G_A with the

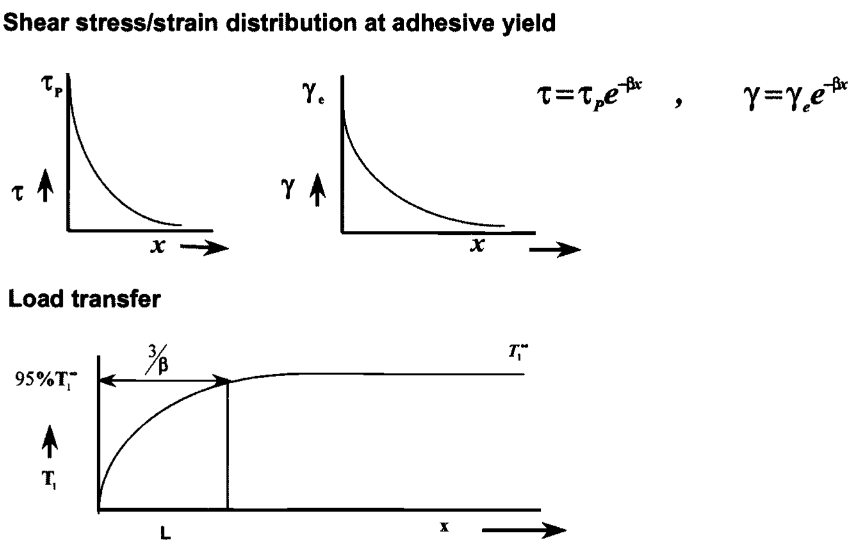

Fig. 9.6 Outcome of the analysis of the skin-doubler joint, assuming elastic behavior in the adhesive.

effective value:

$$\left(\frac{t_A}{G_A}\right)_{eff} = \frac{t_A}{G_A} + \frac{t_2}{G_2} + \frac{3t_1}{8G_1} \tag{9.4}$$

where G_1 and G_2 are, respectively, the shear moduli of the outer and inner adherend.

The maximum load that can be transferred from the inner to the outer adherend per unit width of joint before adhesive yield is given by:

$$T^{\infty}_{1\,\mathrm{max}} = \tau_p \int_0^\infty e^{-\beta x} \mathrm{d}x = \frac{\tau_P}{\beta} \tag{9.5}$$

which is the area under the shear-stress/length curve.

The distance to transfer most (95%) of the load, the load transfer length, is given by:

$$L_{\mathrm{min}} = \frac{3}{\beta} \tag{9.6}$$

If the transfer length is less than $3/\beta$, it is not possible to obtain full load sharing between the adherends.

In the absence of residual stress due to thermal-expansion, mismatch between adherends, and a differential between operating and cure temperatures, the maximum load per unit width (P_{max}) that can be applied at the end of adherend 2 without yielding the adhesive is given by:

$$P_{\max} = \left(\frac{\tau_P}{\beta}\right)\left(1 + \frac{E_2 t_2}{E_1 t_1}\right) \tag{9.7}$$

If residual stresses can arise as a result of the difference in expansion coefficients between, say, a metal panel and a composite doubler, the maximum load that can be applied without yielding the adhesive is given by:

$$P^T_{\max} = P_{\max} + E_2 t_2(\alpha_1 - \alpha_2)\Delta T \tag{9.8}$$

In this equation, ΔT (service temperature—cure temperature) is always negative so that the influence of residual stresses on the maximum load transfer depends on the sign of $\Delta\alpha$ If, for example, adherend 1 is carbon/epoxy and adherend 2 aluminum, then $\Delta\alpha$ is negative and almost equal in magnitude to α for aluminum; taking aluminum as $23 \times 10^{-6}\,^{\circ}\mathrm{C}^{-1}$ and α for a quasi isotopic carbon/epoxy composite to be $4 \times 10^{-6}\,^{\circ}\mathrm{C}^{-1}$.

The result is an increase in the maximum tensile load and a reduction in the maximum compressive load that can be carried by the joint after cooling from the cure temperature. This result is easily explained physically. The inner metallic adherend contracts as the joint is cooled from the cure temperature, producing shear stresses in the adhesive opposing those produced by the applied tensile load. Thus, a significant tensile load must be applied to the joint to overcome this contraction before adhesive starts to be sheared in the original direction. The converse occurs if the applied load is compressive. This topic of residual stress is discussed again later with respect to the double-overlap joint.

9.3.4.2 Elastic/Plastic Model for the Adhesive. The shear stress/joint length relationship in the adhesive, assuming elastic/plastic behavior, is shown in Figure 9.7. In this figure, it is assumed that the adhesive is strained to its full

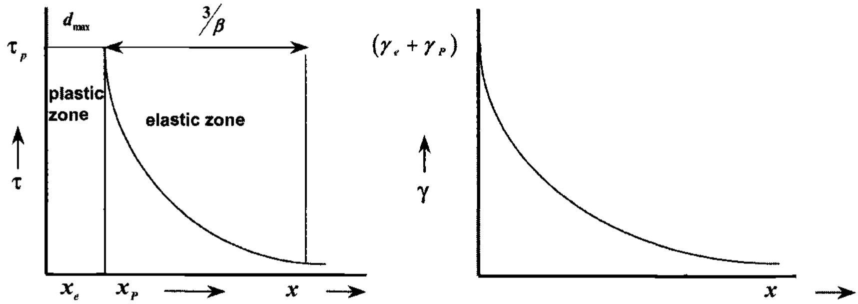

Fig. 9.7 Shear stress/length and shear strain/length distribution in the skin-doubler joint, assuming elastic/plastic behavior in the adhesive.

capacity (see Fig. 9.4), which is:

$$\gamma = \gamma_e + \gamma_P \tag{9.9}$$

As shown in Figure 9.7, a plastic zone length d develops in addition to the elastic zone length $3/\beta$.

Thus, the maximum load transfer capacity is:

$$T_{1\max}^{\infty} = \tau_P \int_0^d dx_P + \tau_P \int_0^{\infty} e^{-\beta x_e} dx_e = \tau_p d_{\max} + \frac{\tau_P}{\beta} \tag{9.10}$$

The length of the plastic zone at failure of the adhesive[11] is given by:

$$d_{\max} = \frac{1}{\beta}\left[\left(1 + 2\left(\frac{\gamma_P}{\gamma_e}\right)\right)^{1/2} - 1\right] \tag{9.11}$$

Using these equations, it can be shown[3] that the maximum load that can be applied to adherend 2 without failing the adhesive is given by:

$$P_{\max} = \left\{\left[2t_A E_2 t_2\left(1 + \frac{E_2 t_2}{E_1 t_1}\right)\right]\left[\tau_P\left(\frac{\gamma_e}{2} + \gamma_P\right)\right]\right\}^{1/2} \tag{9.12a}$$

and, for thermal mismatch,

$$P_{\max}^{T} = P_{\max} + E_2 t_2(\alpha_1 - \alpha_2)\Delta T \tag{9.12b}$$

The area under the shear stress–strain curve for the adhesive appears explicitly within the second square bracket in equation (*9.12a*). This suggests that the load transfer capability should not change significantly with temperature because experimental studies on stress/strain behavior (for ductile structural film adhesives) show that this area does not vary greatly with temperature. The area under the shear stress-strain curve multiplied by the adhesive thickness t_A is a measure of the maximum fracture energy per unit area of crack growth, as discussed in more detail later.

The length required to transfer the load, $T_{1\max}^{\infty}$, is now given by:

$$L_{\min} = d_{\max} + \frac{3}{\beta} \tag{9.13}$$

The minimum transfer length $L_{\min}$ required to transfer T_1^{∞} under arbitrary external load P is [based on equation (*9.10*)] obtained as follows:

$$T_1^{\infty} = \int_0^{\infty} \tau dx = \tau_P d + \frac{\tau_P}{\beta}$$

also:

$$T_1^{\infty} = P/(1 + E_2 t_2/E_1 t_1)$$

and since:

$$L_{min} = d + \frac{3}{\beta}$$

then:

$$L_{min} = P/[\tau_P(1 + E_2t_2/E_1t_1)] + 2/\beta \qquad (9.14)$$

9.3.4.3 End-Termination Shape. The above models have assumed that the doubler (adherend 1) is of constant thickness. However, if its ends are tapered, the peak shear (and peel) stresses can be greatly reduced. This can be achieved by forming an end taper (or scarf) or, as illustrated in Figure 9.8, by stepping. Stepping is the usual configuration for composite joints since it arises naturally when laminating.

An analysis for the stress distribution in doublers with scarfed stepped skin ends is described by Chalkly[13]. Figure 9.8 illustrates part of the model used, and Figure 9.9 is a plot, for the elastic case, of step thickness versus peak shear strain in the adhesive, assuming a step thickness of 0.13 mm and material properties for the composite boron/epoxy; the maximum thickness is 0.65 mm. The peak shear strain asymptotes to a lower bound of about half the peak level after a step length of about 5 mm. Actually, in most practical doubler applications, a step length of approximately 3 mm is used. The peel stress in the adhesive will also be markedly reduced by stepping. Stepping (or scarfing) the ends of the doubler is required in most practical applications, unless the doubler is less than a few plies thick.

A useful estimate of the influence of stepping the ends of the doubler can be obtained using the simple analysis for a constant-thickness doubler, outlined in Figure 9.5. The results are shown as the bounds in Figure 9.9, taking the minimum thickness to be one ply and the maximum thickness that of the full five plies. The step length required to achieve the lower bound is of the order of 4 mm, which is about the minimum length required for full load transfer ($3/\beta$).

It is of note that, for a similar thickness doubler and tapering distance, the analysis shows that the step configuration develops a lower peak shear strain than the scarfed configuration.

9.3.5 Double-Overlap Joint

Figure 9.10 shows schematically one side of a simple double-overlap joint. It is assumed in this diagram that the adherends are of similar (balanced) stiffness, the product of modulus and thickness (Et). At the left end, where the outer adherend terminates, the load distribution is identical to that in the skin-doubler joint shown in Figure 9.5. At the right end, where the inner adherend terminates, the load remaining in the inner adherend is transferred to the outer adherend—this configuration is Figure 9.5, inverted.

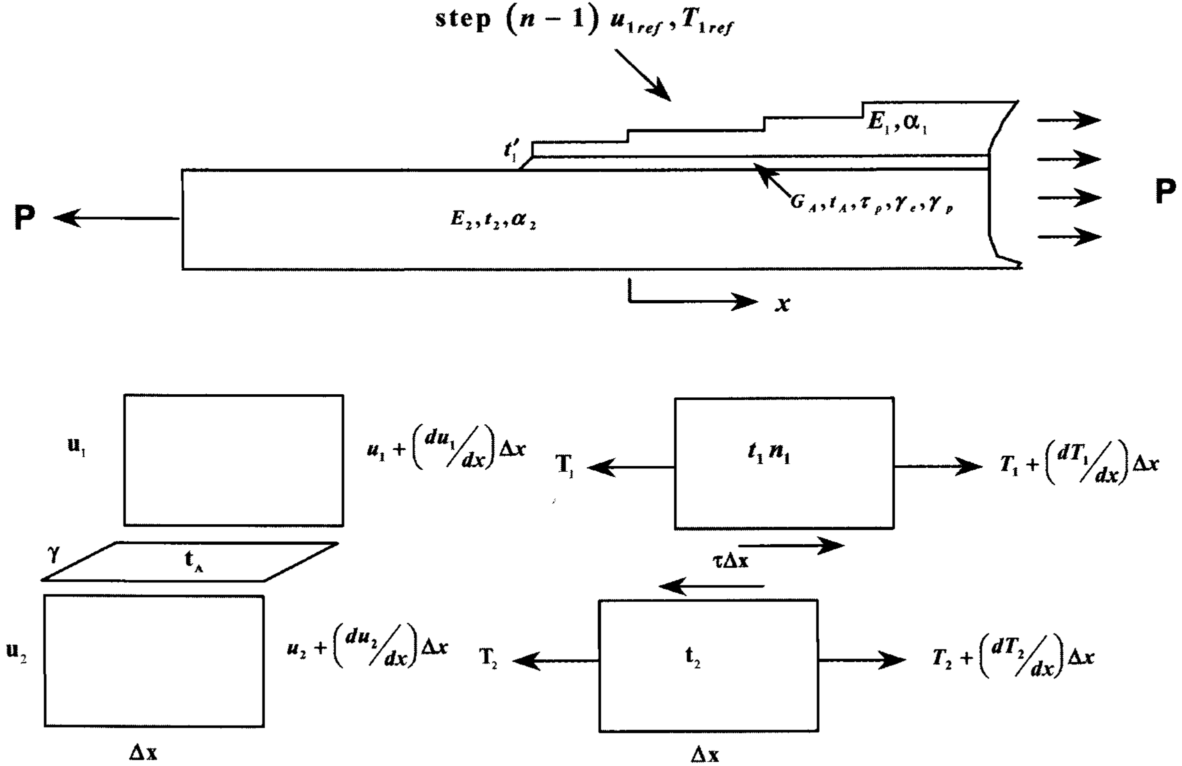

Fig. 9.8 Skin-doubler joint with stepped ends, showing part of the analytical model.

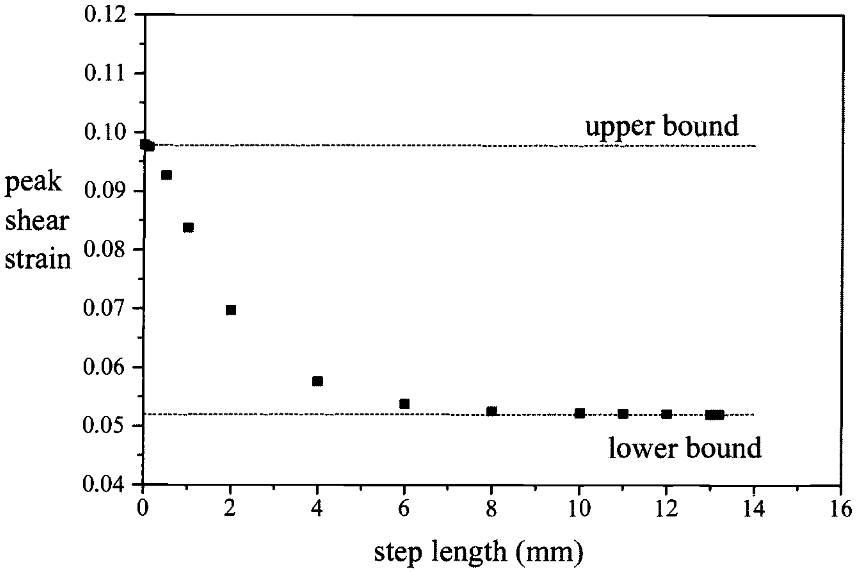

Fig. 9.9 Outcome of the analysis of the skin/doubler joint with stepped ends, assuming elastic behavior of the adhesive. The upper and lower bounds assume full thickness or thickness of one ply. Taken from Ref. 13.

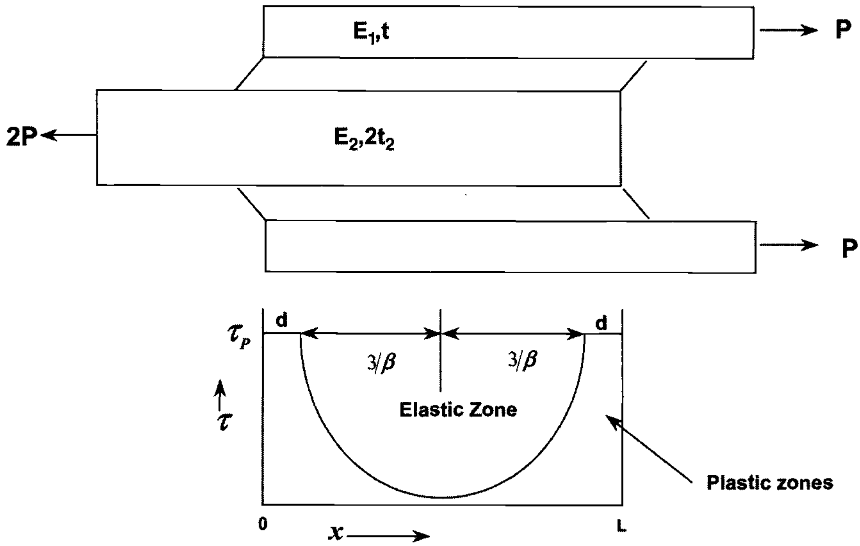

Fig. 9.10 Double-overlap joint showing shear stress/length distribution in the adhesive, assuming elastic/plastic behavior in the adhesive and stiffness-balanced adherends.

9.3.5.1 Overlap-Length, Balanced Joint. Figure 9.10 shows schematically the shear stress distribution in the adhesive in the double-overlap joint. To minimize the weight penalty in the joint, it is desirable to use the shortest possible overlap length, with some allowance for defects and damage. The minimum overlap length, $L_{\min}$, for $P < P_{\max}$, is estimated as follows.

We have that:

$$L_{\min} = 2d + 6/\beta \quad \text{minimum transfer length}$$

and:

$$T_{1\max} = 2\tau_P d + 2\tau_P/\beta = P \quad \text{maximum load transferred}$$

so:

$$d = P/2\tau_P - 1/\beta$$

For adherend 1, failure $P = P_u = \sigma_{1u} t_1$.

Thus,

$$L_{\min} = \frac{\sigma_{1u} t_1}{\tau_P} + \frac{4}{\beta} \tag{9.15}$$

Alternatively, for composites, it is usual to work to an ultimate design strain level ε_u, typically 4000 microstrain. The strain capacity to failure exceeds this value markedly, typically up to 13,000 microstrain, but this much more modest value allows for strength reduction due to damage and stress concentrations.

Then (per unit width of the joint):

$$P_u = E_1 \varepsilon_u t_1 \tag{9.16}$$

Here P_u is half the total load applied to the joint. Then:

$$L_{\min} = E_1 \varepsilon_u t_1/\tau_P + 4/\beta \tag{9.17}$$

In this case, since $E_1 = E_2$ and the total thickness of the outer adherends equals the inner adherend $= 2t$, β is simplified in equation (*9.3*) to $\beta = \sqrt{2G_A/t_A E t}$.

However, longer overlaps are highly desirable (if cost and weight penalties are not too great) because they provide high levels of damage tolerance to voids and other flaws. It is important that the minimum value of shear stress $\tau_{\min}$ not exceed about $\tau_P/10$, which approximately corresponds with the elastic trough of length $3/\beta$.

As overlap lengths decrease below $L_{\min}$, the minimum shear stress in the elastic trough $\tau_{\min}$ gradually increases until it becomes uniform (τ can reach a maximum level of τ_P when the whole adhesive layer becomes plastic). This results in 1) a loss of damage tolerance because the joint strength is sensitive to bond length, and 2) a susceptibility to creep strain accumulation.

9.3.5.2 Stiffness Imbalance. The load-carrying capacity of a double-overlap joint is estimated as follows.

For the right-hand end, from equation (*9.12*):

$$P_{\max} = \left\{\left[2t_A E_1 t_1\left(1 + \frac{E_1 t_1}{E_2 t_2}\right)\right]\left[\tau_P\left(\frac{\gamma_e}{2} + \gamma_P\right)\right]\right\}^{1/2}$$

Similarly, for the left-hand end:

$$P_{\max} = \left\{\left[2t_A E_2 t_2\left(1 + \frac{E_2 t_2}{E_1 t_1}\right)\right]\left[\tau_P\left(\frac{\gamma_e}{2} + \gamma_P\right)\right]\right\}^{1/2} \tag{9.18}$$

The strength is given by the lower of these two values.

For a stiffness-balanced joint $E_1t_1 = E_2t_2 = Et$, so

$$P_{\max b} = 2\left[t_A E t \tau_P\left(\frac{\gamma_e}{2} + \gamma_P\right)\right]^{1/2} \tag{9.19}$$

If an unbalanced joint is created by reducing the stiffness of one of the adherends, let $S = E_1t_1/E_2t_2$ or $= E_2t_2/E_1t_1$, whichever is the smaller. Then:

$$P_{\max un} = \left\{\left[2t_A S E t(1 + S)\right]\left[\tau_P\left(\frac{\gamma_e}{2 + \gamma_P}\right)\right]\right\}^{1/2}$$

then:

$$\frac{P_{\max un}}{P_{\max b}} = \frac{\sqrt{2S(1+S)}}{2} \tag{9.20}$$

Because this ratio must always be less than 1, the unbalanced joint is always weaker than the balanced joint. The weaker end of the joint is where the lower stiffness adherend extends. This is intuitively obvious because this is the end with the greater deformation of the adherend, resulting in the larger shear deformation in the adhesive.

9.3.5.3 Thermal-Expansion Mismatch. As with the skin-doubler joint, residual stresses have a significant influence on the strength of the double-overlap joint. Unlike the skin-doubler joint, the residual stress has a different effect at each end of the joint, being beneficial at one end and detrimental at the other,[7] as illustrated in Figure 9.11.

For a balanced joint the load-carrying capacity is given by the smaller value of:

$$P_{\max} = 2\left[t_A E t \tau_P\left(\frac{\gamma_e}{2} + \gamma_P\right)\right]^{1/2} \pm Et\Delta\alpha\Delta T \tag{9.21}$$

where $\Delta\alpha$ is the difference in expansion coefficients between adherends.

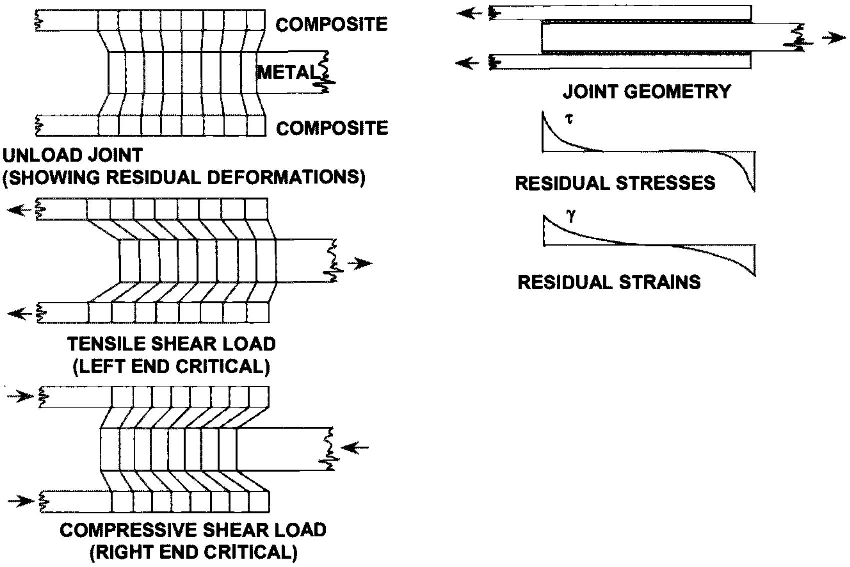

Fig. 9.11 Schematic illustration of the effect of thermal expansion mismatch in a double-overlap joint. Taken from Ref. 7.

The situation is somewhat more complicated when there is both stiffness imbalance and residual stress due to thermal-expansion mismatch. The load-carrying capacity of the joint in this case is given by:

$$P_{\max} = \left\{\left[2t_A E_1 t_1\left(1 + \frac{E_1 t_1}{E_2 t_2}\right)\right]\left[\tau_P\left(\frac{\gamma_e}{2} + \gamma_P\right)\right]\right\}^{1/2} + E_1 t_1(\alpha_2 - \alpha_1)\Delta T \quad (9.22a)$$

or

$$P_{\max} = \left\{\left[2t_A E_2 t_2\left(1 + \frac{E_2 t_2}{E_1 t_1}\right)\right]\left[\tau_P\left(\frac{\gamma_e}{2} + \gamma_P\right)\right]\right\}^{1/2} + E_2 t_2(\alpha_1 - \alpha_2)\Delta T \quad (9.22b)$$

9.3.5.4 Peel-Strength Limitation on Strength and Methods of Alleviation. The approach used by Hart-Smith[8] to estimate peel stress is outlined in Figure 9.12. The origin of the peel stress is the horizontal shear stress, which results from load transfer along the bond line at the ends of the joint. Because there are no complementary vertical shear stresses at this point, the unbalanced horizontal shear stress produces a bending moment that acts to bend the outer adherend away from inner adherend. To react-out this bending moment,

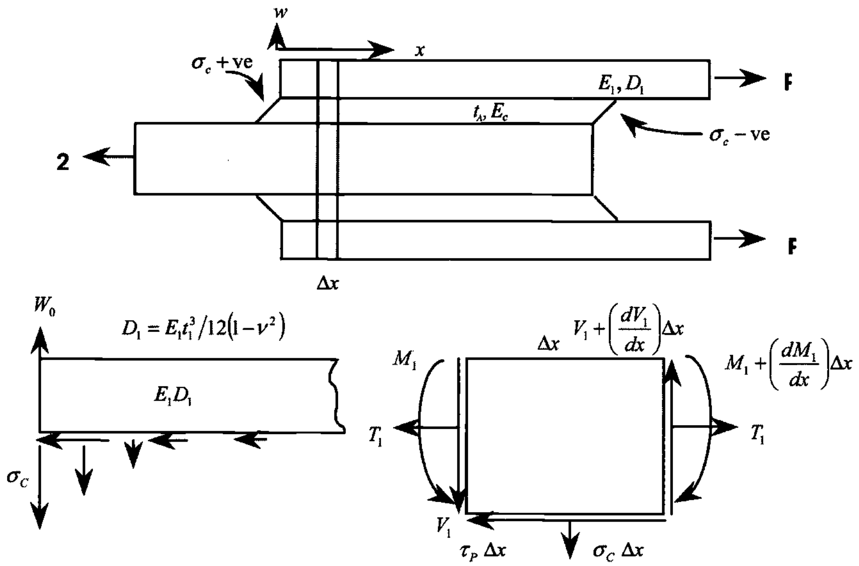

Fig. 9.12 Model analysis for peel stresses.

through-thickness (peel stresses) develop in the adhesive. Note that while the peel stress at the ends of the joint is positive for tensile loading, it is negative (compressive) for compressive loading, so not usually of concern.

Hart-Smith[14] also provides detailed treatment of design to minimize peel stresses in several other types of bonded joint. The simplifying assumption made in most of these analyses is that the shear stress at the ends of the adherends is constant at τ_p, the shear yield stress in the adhesive.

From the analysis outlined in Figure 9.12, the result is that the peel stress, σ_c, is given by:

$$\sigma_c = \tau_p\left(\frac{3E'_C t_1}{E_1 t_A}\right)^{1/4} \tag{9.23}$$

where E'_C is the effective transverse stiffness of the joint, including the adhesive and adherends. From this relationship, it can be seen that σ_c increases with increasing thickness of the outer adherend and is reduced with increasing modulus of the outer adherend and increasing thickness of the adhesive layer. Peel stresses can be alleviated by control of these parameters as well as by the various approaches illustrated in Figure 9.13. The presence of adhesive spew, as discussed in the next section, can also significantly reduce peel stresses.

Metallic adherends have very high peel strength, therefore peel failures occur in the adhesive layer. In contrast, peel is much more of a concern with composite

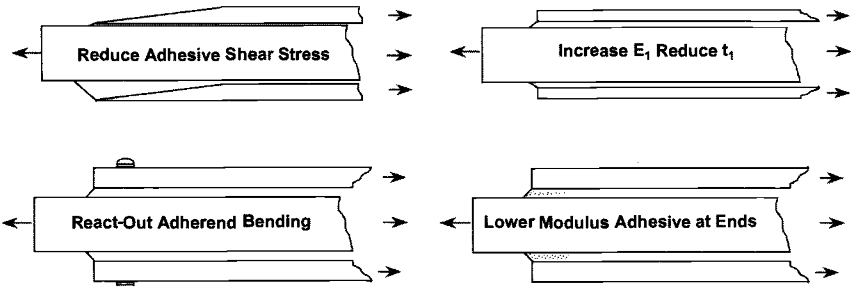

Fig. 9.13 Some methods for alleviating peel stresses.

laminates because they have much lower peel strength than do structural adhesives. Failure can occur in the plies close to the bond surface, or even in the resin-rich layer on the composite surface if this is not removed before bonding.

Comparison of peel resistance of composites can be made more conveniently on the basis of the relative mode I (opening or peel mode) fracture energy. This approach is described later.

9.3.5.5 Adhesive Spew. As mentioned previously, in practical joints a fillet or spew of adhesive forms from adhesive squeezed out during the bonding process. Unless removed by machining, the spew forms part of the geometry of the joint and reduces the maximum shear and peel stresses at the ends of the joint. The spew also acts as a barrier to the ingress of fluids from the operating environment in this critical region of the joint. Thus, removal of the spew, as is sometimes done for cosmetic reasons, is very bad practice.

Classical analytical approaches cannot satisfactorily model this region, so finite element procedures are appropriate. The influence of the spew on stress distribution has been studied in some detail,[10,15] modelling it as a 45° triangle of varying size. In reality, the shape of the spew can vary considerably and can contain significant porosity.

It is found that, within the bond line away from the ends, the principal stresses are tension and compression of equal magnitude—showing that, as predicted by analytical procedures, the adhesive is in a state of pure shear. Within the spew, the principal stress is aligned approximately parallel to the angle of the fillet and is predominantly tensile.

It is predicted and found that for relatively low ductility adhesives, brittle failure occurs in the spew at right angles to the principal tensile stress. The maximum stresses occur very close to the corner of the adherend edge (if sharp) and result in failure at this point. Compared with the failure stresses with no fillet, the maximum shear and peel stresses are reduced by approximately 20% or 30%. A considerable further reduction in peak stresses (about 30%) is obtained by rounding off the corner of the adherends.

In the case of adhesives having significant ductility, it is shown that plastic deformation initiates at these points of high stress.[10]

One approach that considers adhesive spew and ductility[16] correctly predicts the experimentally observed effect of adhesive thickness. Most other theories (finite element as well as analytical) predict that the joint becomes stronger with increasing thickness, in contrast to the observed behavior.

It is assumed that failure occurs when the adhesive layer yields along the full length of the joint. Thus, once the joint is fully yielded (globally yielded), it can carry no further load, and failure ensues. It is shown that although yielding occurs at lower loads in a thin adhesive layer, it spreads more rapidly in a thick adhesive layer—because of lower constraint and more uniform stress distribution.

9.3.6 Effects of Defects in Lap Joints

Considerations have so far been confined to idealized joints having a uniform adhesive layer and uniform adherends. However, in real joints, manufacturing defects and service damage defects occur in the adhesive layer and should be taken into account in the analysis to assess their effect on strength. These defects include local disbonded regions, porosity, and locally thinned regions. The effects of such defects are addressed by Hart-Smith[17] and will be briefly outlined here with respect to the double-overlap joint. The effects of defects can also be evaluated using a fracture mechanics approach, as described later.

Provided the joint is otherwise sound, the effect of local disbonds at the ends of the double-overlap joint is simply to reduce overlap length. Thus, as long as the overlap length is greater than the minimum, no reduction in strength should occur.

A small region of disbond at the center of the joint would have no effect if the overlap length is large. Even if the overlap length were of the minimum length, the effect of the disbond would not be great because only a small proportion of the load is transferred through this region.

Porosity up to a few percent appears to have relatively little effect on static strength of the joint, even when located in the critical load transfer zone at the ends of the joint. It appears that the discrete ligaments between the pores act independently and do not link up to significantly reduce the shear strain capacity of the adhesive. To model the effect of porosity in the joint, it may be sufficient to reduce the effective shear modulus, G_A, the shear yield strain γ_e, and the strain capacity, γ_P The actual values used could be obtained analytically or experimentally. Cyclic loading may be of concern because the voids may link up and form a major disbond. This aspect is under investigation, but is unlikely to be of concern for most practical joints because of conservative design. However, fatigue may be much more of a concern in repair applications, where safety margins are often much lower.

Although it appears that limited porosity may not be of concern in a structural sense, durability problems may arise in service due to the easier path to the bond interface for moisture or other aggressive agents.

During manufacture, excessive adhesive flow may occur out of the ends of a joint. This situation arises because at the ends of the joint there is little resistance to flow of the adhesive and also because locally high pressures can arise in this region. In an extreme case most of the adhesive may be expelled, leaving only a very porous adhesive layer or, in the case of a structural film adhesive, a porous adhesive plus carrier.

Because very high strains will arise in the adhesive—leading to early failure—it is appropriate to consider this region a local disbond. Provided the overlap length is sufficient and tapering of the ends is not required, little loss of joint strength should result. However, disbonded regions at the ends of the joint, although not detrimental initially, can allow ingress of aggressive agents from the environment and so pose a durability problem.

9.3.7 Step-Lap Joint

The step-lap joint is essentially a series of overlap joints and is analyzed as such. Figure 9.14 is an outline of the simple one-dimensional analytical model.[9]

As with the overlap joint, the stepped-lap joint has a non-uniform shear stress distribution with high stresses at the ends of the each step. With correct design, the step-lap joint is capable of joining adherends of any thickness. It is

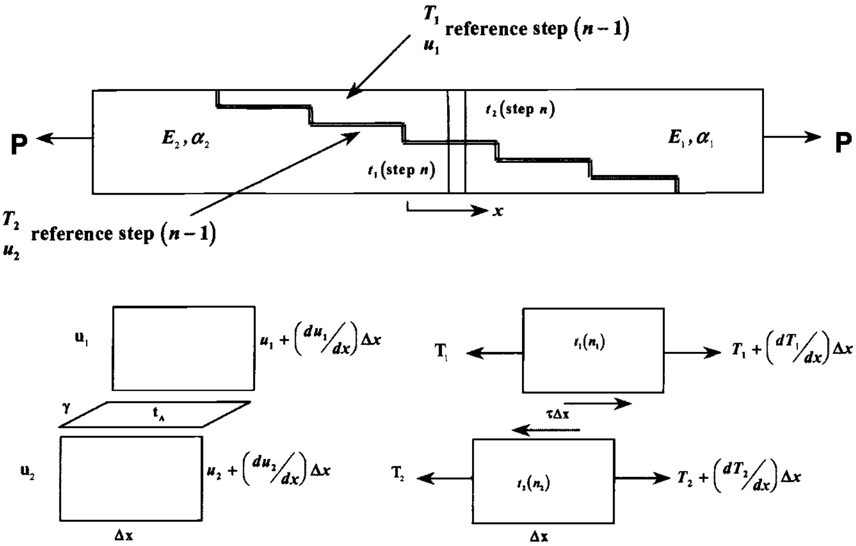

Fig. 9.14 Step-lap joint showing model for analysis.

particularly well-suited to joining laminated composite components because the step-lap configuration is readily produced by the laminating process.

Design of step-lap joints is considerably simplified using the software such as the programs listed in Table 9.2.

To maximize the load-carrying capacity of a stepped-lap joint, it is not sufficient just to increase the length of the steps, because the load-carrying capacity does not increase indefinitely with length. To increase load capacity, it is necessary to increase the number of steps. Furthermore, to avoid overloading thin end steps, it may actually be necessary to reduce their length.

Peel stresses are not usually a problem with step-lap joints because of the alignment of the primary loads and the small thickness change at the ends of each step.

One of the best-known examples of a step-lap joint is the wing-skin-to-fuselage attachment used in the F/A-18 aircraft, shown in Figure 9.15, consisting of (AS3501-2) carbon/epoxy skins bonded with adhesive FM300 to titanium alloy 6Al-4V. Similar joints are used to join boron/epoxy to titanium alloy for the empennage of the F-14 and F-15 aircraft As explained earlier, titanium alloy is used as the metallic component of the joint because it has a low thermal expansion coefficient (around 9×10^{-6} °C^{-1}) and (unlike aluminum alloys) is not prone to galvanic corrosion when in electrical contact with carbon fibers.

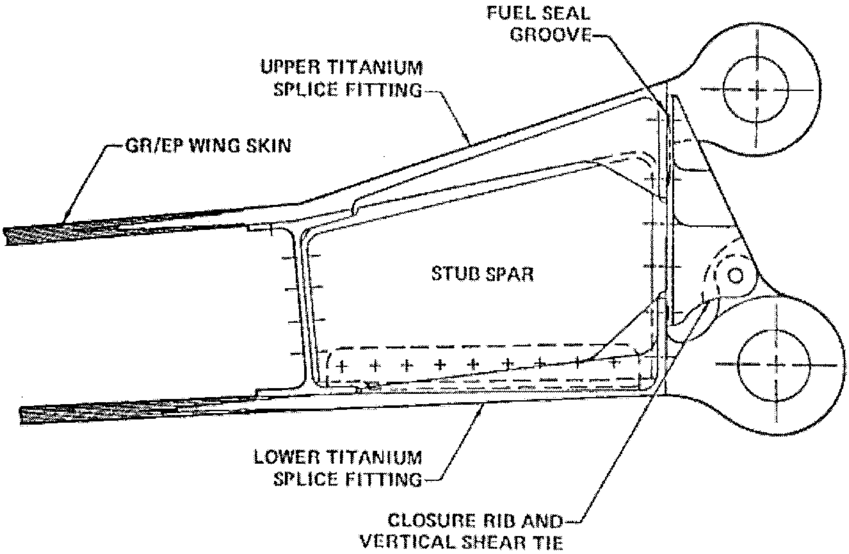

Fig. 9.15 Schematic illustration of the step-lap joint used to attach the carbon/epoxy wing skin to the titanium alloy fuselage attachment lug of the F-18 military aircraft.

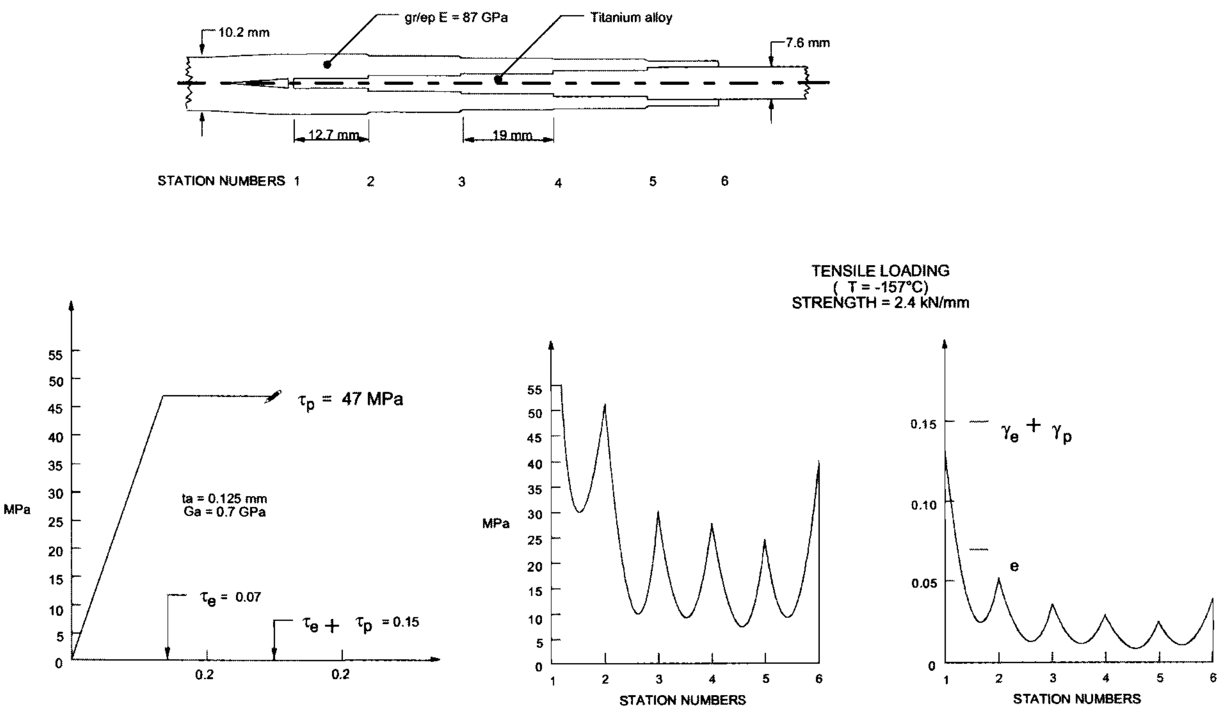

Fig. 9.16 Shear stress as a function of length and step position for a step-lap joint similar to that used in the F-18 aicraft. Taken from Ref. 8.

Figure 9.16 shows the predicted shear-stress distribution for the F/A-18 step-lap joint.

The manufacturing process for step-lap joints is as follows:

- Machine the titanium-alloy wing-root fitting to form the inner step-lap
- Surface-treat and prime the fitting to ensure durable bonding (bonding aspects will be discussed later)
- Apply a layer of adhesive to the lower surface of the fitting
- Place the fitting onto a carbon/epoxy lay-up already in place on the tool—this forms the lower half of the wing skin
- Place adhesive on the top of the fitting
- Lay-up the top half of the wing skin over the lower half of the skin and the fitting

Finally, the whole component is bagged and cured in an autoclave. In this process, it is most important that the plies be correctly positioned. If they are too long or too short for the step, they will cause out-of-plane distortion of the succeeding plies. The result of poor ply placement is development of transverse stresses, leading to the initiation and propagation of delaminations, which will degrade or ultimately cause failure of the joint.

9.3.8 Scarf Joint

Scarf joints (Fig. 9.17) are used mainly for repairs to composite structures, and are therefore discussed more fully in Chapter 10. A simple strength-of-materials

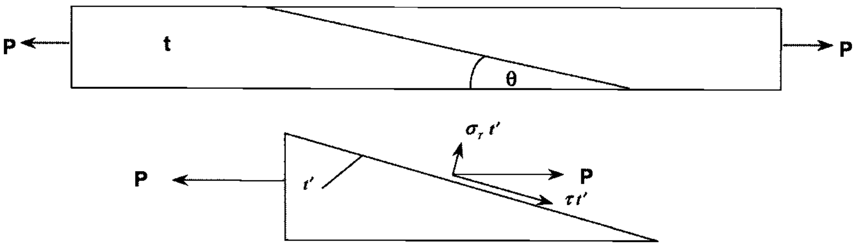

$$t' = t/\sin\theta$$

$$\sigma_T = P\sin^2\theta/t \qquad \tau = P\sin\theta\cos\theta/t$$

so $\quad \sigma_T/\tau = \tan\theta = \theta\text{(radians)}$

for adherend failure before adhesive yield

$$P_{max} = \sigma_u t < \tau_p t/\sin\theta\cos\theta$$

thus $\quad \theta < \tau_p/\sigma_u$ (radians)

Fig. 9.17 Simple strength of materials analysis of a scarf joint.

analysis (based on resolution of stresses and areas), as shown in Figure 9.17, provides a reasonably close estimate of the shear stress in scarf joints where the stiffnesses and expansion coefficients of the adherends are similar,[18] as is generally the situation in a repair. The adhesive is assumed to undergo only elastic shear stress/strain behavior. This is a reasonable assumption in most cases because general yielding is generally not acceptable in a scarf joint for reasons discussed later.

The analysis predicts a uniform shear stress in the adhesive layer given by:

$$\tau = \frac{P \sin\theta \cos\theta}{t} \tag{9.24}$$

and a uniform normal stress in the adhesive given by:

$$\sigma_T = \frac{P \sin^2\theta}{t} \tag{9.25}$$

The ratio of normal stress to shear stress is given by:

$$\frac{\sigma_T}{\tau} = \tan\theta = \theta \text{ (radians)} \tag{9.26}$$

Thus, for a taper angle of 5°, the ratio is <0.1, showing that the normal stresses are negligible.

For adherend failure before adhesive yield, we have that:

$$P_{\max} = \sigma_u t \leq \frac{\tau_p t}{\sin\theta \cos\theta} \tag{9.27}$$

Thus:

$$\theta < \frac{\tau_p}{\sigma_u} \tag{9.28}$$

It will be shown in Chapter 10 that, for typical repair applications, this requires a θ of about 3°.

The uniform shear stress in a balanced scarf joint is beneficial in that the strength of the joint is not limited by local high-stress concentrations at the ends, as in a lap joint. Thus, the load-carrying capacity of the joint increases in proportion to the thickness of the adherends so that, at least in principle, the thickness of material that can be joined is unlimited. However, because there is no elastic trough to limit continuous deformation under prolonged loading, creep leading to eventual failure must be expected if the effective adhesive shear yield stress is reached. Further, joint strength will be sensitive to damage to the tapered edge.

In practice, because of the viscoplastic nature of the adhesive, there is probably no lower limit to the adhesive yield stress under prolonged loading. The reduced yield stress and increased time-dependent behavior imposes a limitation on the allowable load in scarf joints under hot/wet conditions. Thus, design must be based on conservative estimates of elastic properties.

If the adherends are dissimilar in stiffness and/or thermal expansion properties, as in a composite-to-metal joint, a much more complex analysis will be required; part of the model for the one-dimensional elastic analysis[3] is shown in Figure 9.18. This analysis can be based on elastic or elastic/ideally plastic behavior in the adhesive. Table 9.2 provides details on computer programs for analyzing scarf joints.

The net result of the analysis for joints with adherends with different stiffnesses or thermal expansion coefficients is that the shear stress in the joint is no longer uniform. Assuming elastic behavior in the adhesive, it is found that the shear stress concentration, maximum-adhesive-stress/minimum-adhesive-stress (unity for a balanced joint), asymptotes to the lowest adherend stiffness ratio. The effect of adhesive plasticity is to extend the length over which the stress ratio is unity.

The effect of thermal expansion mismatch (stiffness-balanced adherends) is more complex with the shear stress concentration rising and falling with increasing scarf length; at large lengths (very small θ) the ratio approaches unity, as for no thermal mismatch.

9.3.9 Materials Aspects

Bonded joints, composite/composite or composite/metal, are made by secondary bonding or cocuring. In secondary bonding, the components of the joints are first manufactured and are then bonded with a structural adhesive in a secondary operation. In cocuring the joint, the component is cured along with the adhesive during the bonding process. In some all-composite joints, the adhesive is omitted during a cocure, the matrix (resin) being relied on to provide the bond.

The advantage of secondary bonding is that both joint components are processed under ideal conditions and can be inspected before bonding. The advantages of cocuring are that the process is reduced by one step, the critical adherend/adhesive interface is effectively removed and very good dimensional control is possible—even in very complex joints.

9.3.9.1 Structural Adhesives. Most structural adhesives are based on epoxies because these form strong bonds to most suitably prepared substrates, and particularly to high-energy substrates such as metals. Epoxies exhibit little shrinkage during cure, minimizing residual bond-line stresses. Also, because only small amounts of volatiles are emitted during cure, they require only relatively low pressures.

However, even though epoxies have relatively high strength and stiffness and many other desirable properties, they are too brittle to be used in their unmodified form as structural adhesives. Thus, as described in Chapter 4, various approaches

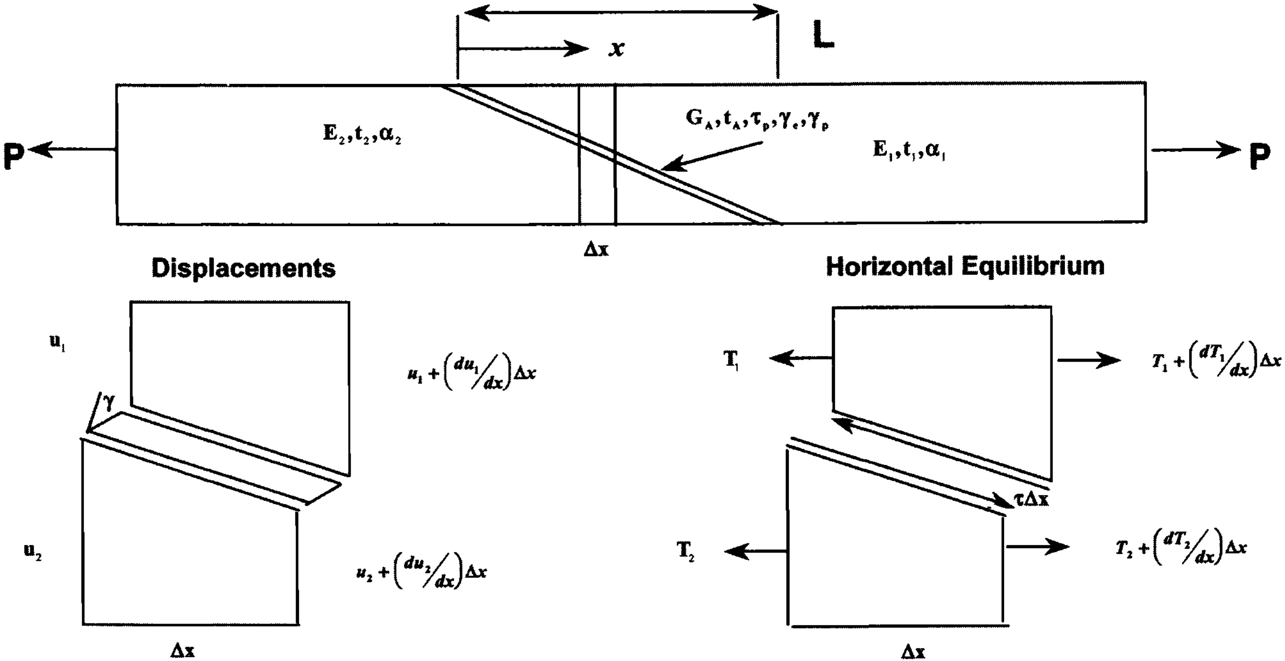

Fig. 9.18 Model for analysis of a scarf joint.

are used to provide toughening, including the formation of a solid solution with a more ductile polymer, precipitation of an elastomeric second phase, and development of an interpenetrating polymer network.

Adhesive forms. Structural adhesives are generally available in two main forms—pastes and film. Paste adhesives are usually of two-component form (i.e., resin and hardener), which are mixed together just before use. In this form, they have the advantage that grades that cure at ambient temperature can be used—also, in most systems, there are no major life limitations before the mixing takes place.

Paste adhesives can also be single component. In this case, the curing agent is premixed with the adhesive. Only adhesives curing at elevated temperature can be stored in this form, and refrigeration is required to provide a reasonable storage life.

Film adhesives are usually formed by coating a fine woven cloth or random mat with the adhesive resin system, which is subsequently partially cured (advanced or staged) to increase viscosity. The fibers generally used for the carrier are polymers such as polyester or nylon; however, glass fibers are also used, mainly with high-temperature adhesives. The resultant film is packaged between release film.

The high-resin viscosity produced by staging prevents resin flow during storage and during the initial stages of bonding when the film is placed on the adherend surface. The degree of staging also determines the level of tack (stickiness) that is available to hold the adhesive and adherends in place before cure.

The carrier in structural film adhesives serves several purposes, including:

- Providing mechanical strength to the uncured (actually, part-cured) adhesive to aid handling
- Controlling flow and thus preventing over-thinning of the adhesive during joint formation
- Providing an insulating layer in the event of complete resin squeeze-out—this is important where carbon/epoxy adherends are bonded to a metal such as aluminum because electrical contact can result in severe galvanic corrosion of the aluminum

Film adhesives are widely exploited in the bonding of aircraft structures. Generally, they provide much higher strengths than the corresponding paste adhesives. Some other important advantages include:

- Ease with which the adhesive can be placed on the adherend surface
- Avoidance of the need for accurate weighing and mixing
- Avoidance of mess (compared with paste adhesives)
- Minimization of entrapped air and volatile materials (from solvent residues)
- Ability to hold adherends in position during cure

In addition, film adhesives assure a higher level of process and therefore quality control.

Disadvantages of film adhesives include high cost, the need for relatively high pressures (compared with single-component paste adhesives) to ensure adhesive flow, high temperatures for cure, and the need for low-temperature storage. Cure temperatures, depending on the hardener system, vary from ambient to around 180 °C, and pressures from zero for paste adhesives to 100–700 KPa for film adhesives.

Factors in the Selection of an Adhesive. Most structural adhesives are capable of bonding the adherends of interest, provided suitable surface treatments can be applied. However, if only very simple treatments are possible for economic or other reasons—such as in a repair application—certain types of adhesive may be favored. This is particularly the case if surface contaminants cannot be removed before bonding.

In rare cases, lack of compatibility of the structural adhesive with the adherend can cause problems. For example, the adhesive—or more likely, the solvent in an adhesive—might attack polymeric materials, particularly thermoplastics; acid or basic products from the adhesive, in the presence of moisture, can corrode some metals, with disastrous consequences to bond strength.

As described earlier, the problem of residual stress arises when joining adherends of different coefficients of thermal expansion with an elevated-temperature curing adhesive. This problem is particularly serious when joining metals such as aluminum to fiber composites such as carbon/epoxy where expansion coefficient mismatch is very large. Residual stress can be minimized by choosing adhesives having the lowest possible cure temperature (if necessary, extending the cure time), a high ductility, and low shear modulus.

Of paramount importance in the choice of an adhesive system is its resistance to attack or degradation in the operating environment. This requirement also applies to the adhesive/adherend interface. Moisture is the main agent responsible for degradation of a metal/adhesive interface whereas many other agents, particularly organic solvents and hydraulic fluids, might attack the adhesive itself.

High temperatures (e.g., above 100 °C) in addition to lowering mechanical properties can cause degradation of the adhesive, due to oxidation or other undesirable chemical reactions. Further, many adhesives exhibit a marked loss in toughness at low temperatures—particularly at temperatures as low as −40 °C, often encountered in aircraft structures. Modified epoxies, particularly some of the film adhesives, have outstanding resistance to loss of toughness at low temperature.

Important economic aspects include the cost of materials, including adhesives; their storage life; the need for expensive surface treatments; the requirement to provide heat and pressure in the cure of the adhesive; and the need for tooling—particularly very expensive items such as autoclaves. Other considerations could include the process time, again favoring adhesives that cure rapidly, and the level of skill required by the personnel in the use of the adhesive. Avoiding the need for accurate mixing of components can save time and the danger of mistakes but often involves the use of adhesives with limited shelf lives.

9.3.10 Assessment of Adhesive Stress/Strain Properties

Toughened epoxy-based film adhesives are generally used to form structural joints for aircraft applications, although paste adhesives are also used for some applications, particularly for repairs. Two film adhesives, FM73 and FM300 (by Cytec Engineered Materials Inc.), are used here as examples of typical adhesives used in composite-to-composite and composite-to-metal bonding. The FM73 and FM300 systems cure at 120 °C and 180 °C, respectively.

Adhesives are qualified for aerospace applications by a range of tests prescribed in ASTM, and the results of these tests are provided in the manufacturers' data sheets. The main joint test specified in these data sheets is the (unsupported) single-overlap joint, similar to that shown in Figure 9.2, with aluminum alloy adherends. The specimens are exposed to a wide range of environmental conditions and tested over a range of temperatures. However, the single-lap joint test, because of severe secondary bending caused by the loading eccentricity, is essentially a combined peel/shear test, therefore it does not provide useable shear stress/strain data, although it does provide very valuable comparative properties, including information on environmental durability.

Thus, to provide useful design data on adhesive shear stress/shear strain behavior for use in joint design, tests based on model joints that produce nominally uniform pure shear stress in the adhesive layer have been developed. Generally, there are significant differences between the results obtained from the various tests, and even between similar tests when undertaken by different laboratories. However, variability can be expected for several reasons, including:

- Properties are sensitive to strain rate, because the adhesive is viscoelastic (or viscoplastic).
- Tests differ in the uniformity of stress in the adhesive layer.
- Failure modes differ.
- Residual stresses due to thermal expansion mismatch differ in different test specimens.

The test most used is the thick-adherend, short-overlap shear specimen,[19] mainly because of its relative simplicity. Figure 9.19 is a schematic of this test specimen showing behavior of adhesive FM73 at two temperatures.

Several manufacturers of aerospace adhesive now include stress/strain behavior of the adhesive (usually using the short-overlap shear specimen) in their data sheets. Table 9.3 provides some of the properties used for design purposes.

Although it is tempting to use these plots as though they were as reproducible as a stress-strain curve for a metal, there are several complications, mainly

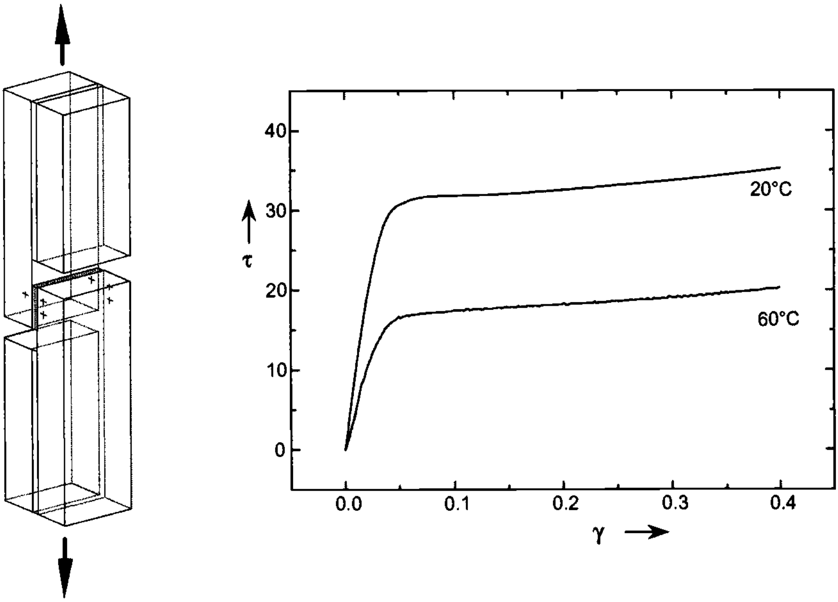

Fig. 9.19 Short-overlap shear specimen and shear stress–shear strain curves for adhesive FM73 at two temperatures obtained using this specimen. Taken from Ref. 20.

associated with time-dependent behavior. Figure 9.20 shows the effects of stress relaxation[20] (constant displacement) on FM73. As may be expected, the curve obtained by plotting the relaxed troughs is similar to the very slow strain rate curve. Thus, a curve obtained by joining the relaxed points could be taken as a master plot for static loading at ambient temperature.

To be useful in the design and analysis of practical joints, the shear stress-strain curve must allow the formulation of simple and consistent failure criteria. Two intuitive failure criteria for elastic/plastic behavior in the adhesive based on the shear stress/shear strain behavior are the plastic shear strain, γ_p, and the shear strain density (e.g., the area under the stress-strain curve to failure).

The failure criteria ideally should be invariant with adhesive thickness. Furthermore, design approaches based on these criteria should be capable of allowing for residual stresses and defects in the bond line and representative loading of the joint. While the above criteria are implicit in the Hart-Smith design approach used here, its validity has yet to be established. For example, it is a concern that the approach does not appear to correctly predict the experimentally observed influence of adhesive thickness. Generally, as mentioned earlier, it is found that (within certain limits) joints get stronger with decreasing adhesive thickness.

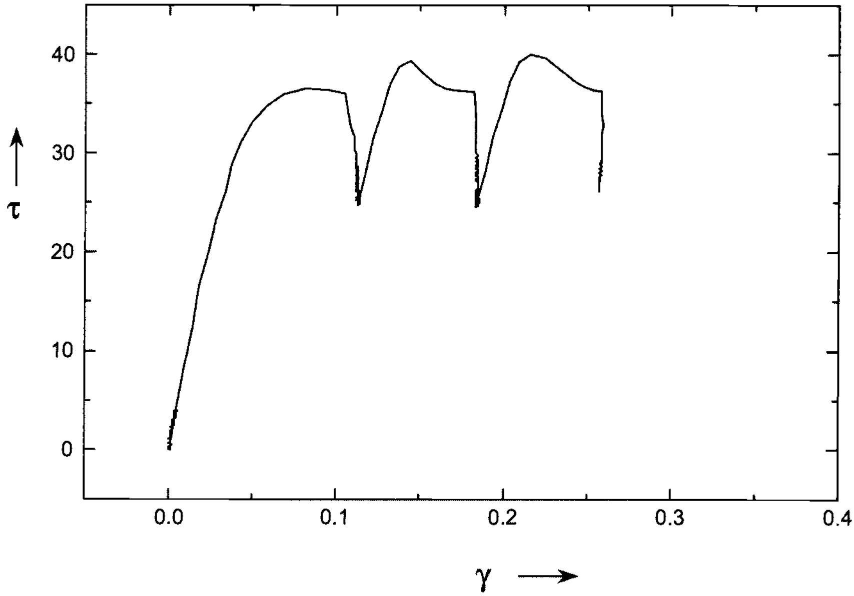

Fig. 9.20 Shear stress/strain relaxation behavior measured using the short-overlap shear specimen.

An entirely different approach to joint design is based on fracture mechanics that assumes the presence of pre-existing flaws, as discussed in the next section.

9.3.11 Assessment of Fracture Energy of Adhesives and Composites

Failure from pre-existing cracks can be categorized into the following basic modes based on the nature of the crack-face displacement: mode I opening or cleavage mode, mode II in-plane shear, and mode III torsional shear. Failure by a mixture of these modes is also possible.

These basic and mixed modes of failure occur in a bonded joint.[21] Generally, for adhesive joints, mode I (peel) is of most concern because this is the mode in which both the adhesive and the composite are weakest.

As may be expected, the fracture behavior of a polymer as an adhesive may differ markedly from that of the bulk material, mainly because of the constraint imposed on the adhesive by the adherends. Furthermore, the crack is constrained to propagate within the boundaries set by the adherends. Thus, while in the bulk material under complex loading, a crack can orient itself to propagate under mode I conditions; this is often not possible in the adhesive layer, so that propagation is forced to occur under mixed-mode conditions.

As previously discussed, various loci for the failure in composites are possible, including:

- In the adhesive layer
- At the adhesive/adherend interface
- In the resin layer near the composite surface
- In the composite surface plies
- Within the adherends

Failure within the adhesive, called cohesive failure, usually represents the maximum level of fracture resistance. Failure at the adherend/adhesive interface is called adhesive failure and represents an off-optimum mode of failure—generally resulting from inadequate pre-bonding surface preparation.

Studies are conducted on the fracture behavior of adhesives in joints for three purposes:

(1) To generate valid comparative data that will aid in the selection of adhesives
(2) To provide data and information that will aid in the development of improved adhesive materials
(3) To provide data to be used in the design of adhesive joints

The energy approach to fracture is based on two parameters:

(1) A mechanical component: the elastic strain energy release rate G in the specimen due to the extension of crack length by unit area. This depends only on the geometry and stiffness properties of the specimen (G_{I}, G_{II}, or G_{III}, depending on the mode of crack propagation).
(2) A materials component: the fracture energy R absorbed by extension of the crack by unit area (also called toughness). This is the materials parameter being measured and is given by the critical value of G at which the crack grows spontaneously ($R = G_{IC}$ for mode I). R is often related to the extent of plastic deformation that can develop at the crack tip, so it can be a strong function of adhesive thickness.[22]

Several tests based on stable crack growth are used to measure the fracture energy of composites in mode I, mode II, or mixed mode. These tests are also used to measure the fracture energy in bonded composite joints.[21]

Some of the most important tests for composites[23] are depicted in Figure 9.21, which also indicates the percentage G_{I}. It was found[24] that lap joint tests were unreliable for measuring fracture energy in bonded joints although, as discussed in the next section, they can be satisfactorily used to measure fatigue properties. To avoid the possibility of failure in the composite rather than in the adhesive, similar tests can be conducted using metallic adherends.

The interlaminar fracture energy of the composite is an order of magnitude lower than that of a structural film adhesive; for example, G_{IC} for the carbon/epoxy composite is around 150 J m^{-2} whereas for adhesives FM73 and FM300 it is, respectively, around 3 kJ m^{-2} and 1.3 kJ m^{-2}. Therefore, if a crack can move

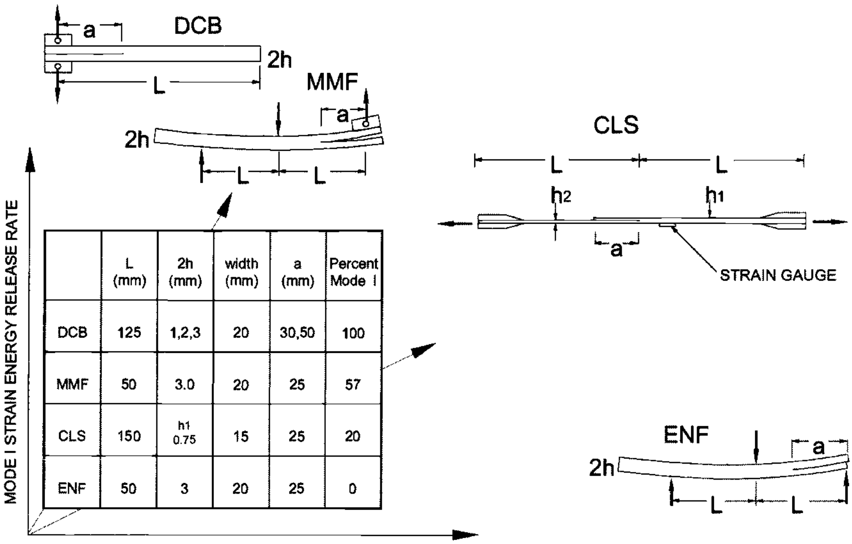

	L (mm)	2h (mm)	width (mm)	a (mm)	Percent Mode I
DCB	125	1,2,3	20	30,50	100
MMF	50	3.0	20	25	57
CLS	150	h1 0.75	15	25	20
ENF	50	3	20	25	0

Fig. 9.21 Types of specimen used for measurement of fracture properties in laminated composites and bonded joints, showing percentage of mode 1, taken from Ref. 23. Note DCB; double cantelever beam, MMF; mixed-mode flexural, CLs; cracked lap shear, and ENF; edge-notched flexural.

from the adhesive layer into the composite or if a crack (delamination) already exists in the composite, failure of the composite surface plies will be the most likely failure mode under most loading conditions. Alternatively, if a layer of matrix resin remains on the composite surface after surface treatment, this may be the preferred path for failure.

As for the design approach based on the shear stress/shear strain behavior, the fracture mechanics approach to be useful must allow for adhesive thickness and residual stresses. In joints designed to minimize peel stresses, it is mainly the mode II behavior that is of interest. Use of G_{IIC} as the fracture criterion is thus an alternative approach to the strain capacity approach previously discussed. Generally, the fracture mechanics approach is to assume the presence of a delamination or disbond just below the size that could be readily found by non-destructive inspection, approximately 1 mm.

The fracture mechanics approach is more useful in the design of joints having a significant mode I (peel) component. In this case, the composite will usually be the most vulnerable component of the joint, therefore strength can be determined by its G_{IC} or by some combination of G_{IIC} and G_{IC} for mixed mode.

For a double-lap joint, it can be shown (based on a simple strength of materials approach and ignoring any peeling effects) that the strength and fracture mechanics approaches to predict joint strength P_{max} result in identical conclusions if G_{IIC} is taken as equal to $t_A \tau_p(\gamma_e/2 + \gamma_p)$ the area under the shear stress–strain curve for the adhesive; see, for example, equation (*9.19*).

For example, using the properties listed in Table 9.3 for adhesive FM73 at ambient temperature with an adhesive thickness of 0.2 mm gives maximum value of G_{IIC} of about 5 kJ m^{-2}, which agrees well with measured values at this adhesive thickness.

The above approach indicates that G_{IIC} should scale linearly with adhesive thickness. However, as previously mentioned due to constraint, it is found experimentally that G_{IC} is generally a non-linear function of adhesive thickness, and a similar situation may be expected to apply to G_{IIC}. Thus, tests are required to measure these parameters at approximately the same thickness as expected in the joint.

9.3.12 Fatigue

Fatigue verification is usually undertaken on critical joints to demonstrate that the joint can carry the ultimate load through its design life, under representative service conditions of stress, temperature, and humidity. The design of such joints is still very far from the point at which the influence on joint performance of aspects such as scale, spectrum stressing, and service environment can be inferred from data on simple specimens (coupons). However, fatigue tests on simple specimen and model joints (such as the short-overlap shear specimen) are often also undertaken at an early stage to screen candidate adhesives and provide design data. Preliminary tests may also be carried out on specimens much more

Table 9.3 Some approximate values for adhesive properties for two typical epoxy-nitrile film adhesives based on the actual shear stress-strain curves (idealized values used in lap-joint calculations will differ considerably, depending on shape of the stress-strain curve and the strain level; see Fig. 9.4)

Adhesive	Exposure temperature (°C)	G_A (GPa)		τ_p (MPa)		γ_p	
		Dry	Wet	Dry	Wet	Dry	Wet
FM73	−55	0.9	0.8	50	56	0.5	0.3
	24	0.8	0.7	32	29	0.9	1.0
	60	0.5	0.4	18	—	1.4	1.4
	82	0.3	—	11	—	1.6	1.6
FM300	−55	—	—	—	—	—	—
	24	0.9	—	42	—	0.9	—
	104	0.5	0.2	21	13	1.3	1.2

Note: $\gamma_e = \tau_p/G_A$.

representative of the actual joint; if these can also provide the design data, they may be used in place of the coupon specimen.

Simple endurance testing of adhesives is also often undertaken using the single-overlap shear specimen. However, for reasons already discussed, this test can provide only comparative data.

For the model joints (which are designed to have uniform shear in the adhesive) repeated cyclic stressing to high plastic strain levels can result in creep failure of the joint after a relatively small number of cycles.[25] This is because cyclic shear strains are cumulative. (If the cycle rate is high, full strain recovery cannot occur during the unloading cycle.) The result is an accelerated creep failure of the adhesive by a *strain ratcheting* mechanism. In practical lap joints, this situation is avoided by maintaining a sufficiently long overlap, so that much of the adhesive remains elastic. The elastic region on unloading acts as an elastic reservoir to restore the joint to its unstrained state preventing the damaging strain accumulation.

Data on crack propagation under loading is most usually obtained from the fracture mechanics-type lap joint tests, as depicted in Figure 9.21, using the edge-notched flexural specimen[26] for mode II, the double-cantilever beam specimen for mode I, and cracked lap-shear specimen for mixed mode.[21] In these tests, the rate of crack propagation in the adhesive is usually plotted as a function of the strain-energy-release-rate range. The empirical relationship between the range of strain-energy-release-rate determined is of the form:

$$\frac{\mathrm{d}a}{\mathrm{d}N} = A\Delta G^n \tag{9.29}$$

where a is the disbond or crack length in the adhesive, N the number of fatigue cycles, and ΔG the range of strain-energy release rate for the relevant mode. The parameters A and n are empirically determined constants. In the mixed-mode specimens, it was found[21] that the better correlation is with the total strain-energy strain range ΔG_T, showing that modes I and II contribute to damage growth. Figure 9.22a shows a typical result for the adhesive FM300.

Comparative studies[27] on several joint types have shown that the values of the crack-growth parameters are similar, indicating the potential value of this approach as a design tool.

For crack growth in airframe aluminum alloys (generally tested under mode I loading), n is of the order of 1.5–3, whereas for the typical structural film adhesive FM300 (film thickness, 0.2 mm), n is close to 5, both under pure mode I and mixed-mode loading.[21] This indicates that disbond growth in these adhesives is rapid. Thinner bondlines due to higher constraint would probably have much higher values of n. For a more brittle adhesive,[28] such as FM400, under mode I loading, n was as high as 12, confirming (the known) poor peel resistance.

For disbond propagation in the composite, n will also be very high because of the brittle matrix and thin effective bond line.

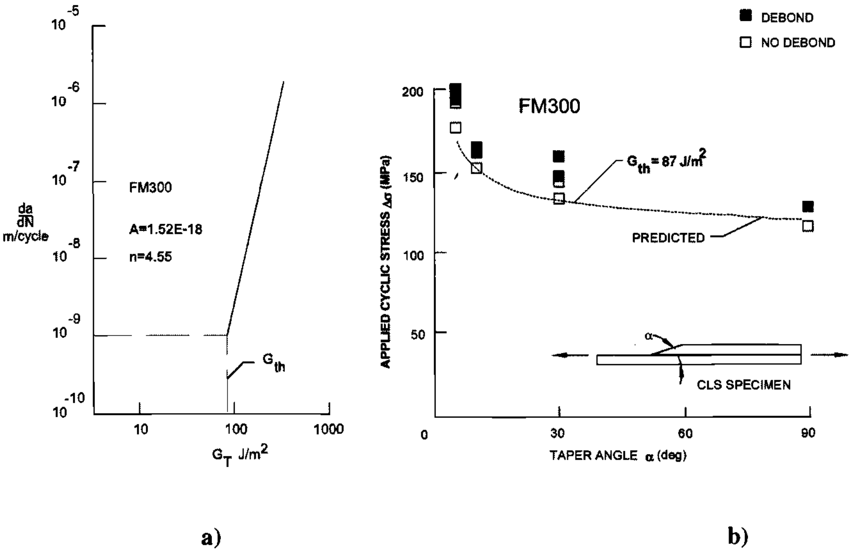

Fig. 9.22 ***a*) Schematic plot of d*a*/d*N* versus ΔG_T based on data for adhesive FM300; *b*) use of data to predict damage growth in CLS specimen with tapered end. Taken from Ref. 21.**

These observations strongly discourage the use of (damage-tolerant) designs based on controlled disbond growth under cyclic loading conditions. Thus, for most of the life of the joint, the design approach must be to hold ΔG below (a conservative estimate of) the threshold for crack initiation, ΔG_{Th}.

An alternative damage criterion for loading, involving mainly mode II crack propagation, is the cyclic strain range $\Delta\gamma$ experienced by the adhesive[29]. This parameter is more convenient to use than ΔG_{II} because it is easier to estimate from a one-dimensional joint analysis, described previously, and automatically includes the influence of adhesive thickness and residual stresses. However, its validity for use in fatigue loading has yet to be proved.

The threshold strain-energy-release-rate range ΔG_{Th} was used as a measure of the cyclic stress level for damage to occur in a (unidirectional) carbon/epoxy cracked-lap specimen bonded with adhesive FM300 or a paste adhesive.[21] The ends of the cracked-lap specimen had taper angles of either 5°, 10°, 30°, or 90°.

The estimated cyclic stress levels for the initiation of damage were compared with the observed level for the various taper angles. It was assumed that damage would grow when $\Delta G_T = \Delta G_{Th}$.

An FEA program was used to estimate G_T for the joint, assuming the presence of a small delamination 1-mm long for the tapered end. The value for ΔG_{Th} was taken as the strain-energy release range for a debond propagation rate of 10^{-9} m cycle^{-1}. For FM300, the value of ΔG_{Th} was found to be 87 J m^{-2} at this propagation rate.

Generally, as shown in Figure 9.22b, the correlation was very good between the predicted and observed cyclic stress levels for disbond growth for the various taper angles, indicating the potential of this approach for fatigue-critical joints having a significant mode I (peel) component. Sensitivity to adhesive thickness and other joint parameters remains to be demonstrated. However, use of the shear strain range ($\Delta\gamma$) in the adhesive as a parameter to assess the threshold for disbond growth may be simpler and equally effective.

9.3.12.1 Failure Modes Under Cyclic Loading.

Surface ply orientation. Generally, the ply configuration (proportion of 0°, ± 45°, 90° and their stacking sequence) is determined by factors other than joint design. However, the strength of the bonded joint may be expected to depend on the orientation of the surface ply. The fatigue strength of the interface is intuitively expected to be a maximum when the interface layer of fibers is oriented in the same direction as the major applied load. This fiber orientation will inhibit any cracks in the adhesive layer entering the weaker (low fracture energy) internal composite interface. Most of the fatigue studies had 0° fibers at the bond interface, and fatigue cracking was generally within the adhesive layer. Fiber orientation will probably have less influence a surface layer of matrix resin is present on the surface because this would become the preferred path for crack propagation.

Studies were conducted on cracked-lap shear specimens [with either film adhesive FM300 or a paste adhesive (EC 3445)] with 0°, ± 45°, or 90° plies at the interface.[30] It was found that fatigue damage with the 0° ply at the interface occurred within the adhesive, as expected from earlier work. However, with a 45° ply at the interface, damage grew both in the adhesive and as a delamination between the ± 45° plies. With the 90° interface, ply damage initiated by transverse cracking in this ply and then grew first by a combination of cracking and delamination in the nearby ± 45° plies and then by delamination between the 0°and 45° plies. The value for ΔG_{Th} was considered to be similar for specimens with the 0° and 45° plies. For the 90° plies, the minimum cyclic stress for cracking was much lower.

This suggests that fatigue resistance of the joints is seriously compromised only when the interface plies are 90°. However, the best practice would seem to be to use 0° plies at the interface because the composite was undamaged in this case.

Temperature effects. Studies using the edge-notched flexural specimen[26] were undertaken to assess the effect of temperature using adhesive FM300K. The specimens were made either by secondary bonding or cocuring. It was found that at ambient and elevated temperature (100 °C) damage growth was almost always in the adhesive. However, at low temperature (− 50 °C) for the secondary bonded specimen (where a layer of matrix resin remained on the surface of the composite), damage grew preferentially in the composite matrix. This mode of failure did not occur in the cocured specimen or in the secondary bonded specimen if the specimen was machined to remove the surface layer.

The value of ΔG_{Th} for the matrix mode of failure was about one third of the value for cohesive failure in the adhesive. This change in mode is attributed to the increase in interfacial shear stress in the matrix layer resulting from the high shear modulus (G_A) of the adhesive at low temperature. The shear modulus of FM300 increases from around 0.5 GPa at 100 °C to about 0.9 at -50 °C. Atmospheric moisture absorbed into the adhesive will reduce G_A further at elevated temperature but cause little change at low temperature.

9.3.13 Moisture Effects

Epoxy and other thermosetting polymers used as a basis of both adhesives and the matrices of composites are hydrophilic and therefore absorb moisture from the atmosphere.[31] Thermoplastic polymers absorb relatively little moisture (they are generally much less polar) but are prone to absorb and be damaged or temporarily degraded by organic solvents. With metallic adherends, water can enter only through the exposed edges of the adhesive. However, with composite adherends having thermosetting matrices, water can diffuse through the composite matrix.

Moisture is absorbed at the surface to a level depending on solubility and relative humidity and diffuses into the bulk of the material. Diffusion can also occur through the carrier fibers if these are polymeric. However, because polymeric carrier fibers are thermoplastic, moisture transport is significantly less than it is through the thermosetting matrix polymer. Water can also enter along interfaces, as discussed later. Unfortunately, of all service liquids (including fuel, engine oil, and hydraulic oils), water causes the most degradation to joints bonded with thermosetting polymers, particularly if one of the adherends is a metal.

Absorbed moisture can:

- Plasticize the matrix, reducing its mechanical properties, particularly at elevated temperature; this is generally reversible on drying. The effect of plasticization could be modelled as a local reduction in G_A and τ_p. For relatively small reductions, joint strength may actually increase as a result of more uniform stress distribution. However, the effect on joint creep and fatigue properties may be detrimental.
- Reduce the glass transition temperature T_g, the temperature at which a dramatic change in mechanical properties occurs; this is reversible on drying. For example, for the adhesive FM73 cured at 120 °C, T_g is reduced from 98 to 81 °C with 3.4% absorbed moisture.
- Damage the adherend/adhesive interface, particularly with high-surface-energy adherends such as metals, by physically displacing the adhesive or by hydrating the surface oxide, as discussed later.
- Produce undesirable residual stresses by causing swelling and cracking of the adhesive; these stresses are usually removed on drying.

- Weaken the joint by leaching out unreacted components in the adhesive. The chemicals released can accelerate attack at the bond interface, for example, by changing the pH at the interface.
- Disrupt the joint at temperatures above 100 °C (e.g., during a supersonic dash) through the formation of vapor.

In addition to absorption and diffusion through the base polymer, which are discussed later, water can diffuse along interfaces such as the adhesive/adherend interface and the adhesive/filler interface. Often interfacial diffusion is more rapid than bulk diffusion, depending on the nature of the interfacial bond. The interface between carrier fiber and adhesive does not, however, appear to be a problem in most systems.

Very rapid transport of water by capillary action (wicking) can occur through regions of interfacial separation (disbonds) and cracks and crazes in the polymer.

9.3.13.1 Diffusion Calculations. Moisture diffusion through thermosetting polymers is generally Fickian.[32] That is, at least to a good first approximation, the (one-dimensional) ingress of moisture for a distance x along a wide joint of length L with impermeable adherends (metals) is given by the relationship:

$$\frac{\partial c}{\partial t} = D\frac{\partial^2 c}{\partial x^2} \tag{9.30}$$

where $c(x, t)$ denotes the moisture concentration at distance x at time t, and D the diffusion coefficient does not vary with moisture concentration. Diffusion is classed as non-Fickian where D varies with moisture concentration, for example, glassy polymers. However, the diffusion coefficient is generally strongly dependent on temperature through the relationship $D = D_o e^{-k/T}$
where D_O and K are constants.

The boundary conditions are that:

$$c(0, t) = c(L, t) = c_0$$

where c_0, the moisture concentration at the boundaries, has a constant value depending on the humidity of the atmosphere and the solubility of moisture in the polymer, and L is the length of the joint.

Typical values for epoxy adhesives at around 40 °C are:

$$D = 10^{-12}\,\mathrm{ms}^{-1} \text{ and } c_0 = 4\% \quad \text{for RH} \approx 100\%$$

For comparison, typical values for carbon/epoxy composites (through thickness diffusion) are:

$$D = 10^{-13}\,\mathrm{ms}^{-1} \quad \text{and} \quad c_0 = 2\% \quad \text{for RH} \approx 100\%$$

Diffusion is slower for the composite because it contains only approximately 40% by volume polymer matrix, which also has a smaller concentration of rubber toughening additions than used in the adhesive.

The capacity of a polymer to transmit water is its permeability, given by the product Dc_0. Thus, the composite is about one order of magnitude less permeable than the adhesive.

A convenient solution to equation (*9.30*), which provides an approximate estimate of moisture concentration c for one end of a long joint, is:

$$c(x,\, t) = c_i + (c_0 - c_i)\left[1 - erf\left(\frac{x}{2\sqrt{Dt}}\right)\right] \tag{9.31}$$

where c_i is the initial moisture content and the error function $y = x/2\sqrt{Dt}$ may be obtained from tables. Table 9.4 provides some values of $erf(y)$.

When c_i, the initial value of moisture, is zero equation (*9.31*) reduces to:

$$c = c_0\left[1 - erf\left(\frac{x}{2\sqrt{Dt}}\right)\right] \tag{9.32}$$

It is useful to note that when $x = \sqrt{Dt}$,$c = c_0/2$. Thus, the time for the moisture level to rise to half of the surface concentration at distance x is given by $t = x^2/D$. For a typical adhesive, assuming zero initial moisture at $x = 5$ mm, half a typical load-transfer length, it would take only 10 months at 40 °C under conditions of high humidity to reach 2%.

It will be shown later[33] that, for metallic adherends, a critical level of moisture appears to exist for chemical attack to occur. Typically (for epoxy bonds to steel) this is of the order of 1.4%, which, for the assumed system, is reached at the 5-mm point in approximately 6 months.

For the case of composite adherends, moisture can simultaneously reach the whole surface by through-thickness diffusion. The rate of diffusion and the final level of moisture away from the edges of the joint is mainly determined by the composite adherend, so the adhesive layer can be neglected.

Table 9.4 Some Values of the Gauss Error Function for a Range of y Values

y	$erf(y)$	y	$erf(y)$
0.0	0.000	0.8	0.742
0.1	0.112	0.9	0.797
0.2	0.223	1.0	0.843
0.3	0.329	1.2	0.910
0.4	0.428	1.4	0.952
0.5	0.521	1.6	0.976
0.6	0.604	2.0	0.995
0.7	0.678	2.4	0.999

Assuming, for example, that the composite adherend has a thickness of 3 mm, the time for the adhesive layer to reach 1.4% at 40 °C (ignoring diffusion in from the ends of the adhesive) is approximately 6 years. Thus, diffusion through the bulk of the composite may not be a major concern. In a real exposure situation involving drying periods[34] by solar heating, the typical maximum moisture content in the composite is generally less than 0.7%.

However, moisture will diffuse more rapidly through the critical tapered-end regions. For example, considering diffusion only through the composite layer of 0.12 mm thick (one ply), a moisture concentration of 1.4% is reached in about 100 hours. Here the combined two-dimensional effect of diffusion through the composite and along the adhesive must be considered and will be significantly worse than with metal adherends.

9.3.13.2 Interfacial Strength Degradation. As mentioned earlier, loss in interfacial strength due to moisture absorption can occur by two major mechanisms:

(1) Physical displacement of the adhesive by water, this occurs where bonding is of a physical nature and the energetics favor the adherend/moisture interface rather than the adherend/adhesive interface.
(2) Chemical disruption of the interface, this occurs where the surface can react with dissolved moisture. Hydration of the metal oxide in bonds involving metallic adherends is the main example of this problem.

The case of physical displacement at the interface may be analyzed by the following simple thermodynamic approach[33] in which only physical forces (e.g., hydrogen bonds) are considered to be acting. Such forces are believed to predominate in many types of adhesive bond.

First, in an inert medium, the work of adhesion is given by:

$$W_A = \gamma_a + \gamma_s - \gamma_{as} \tag{9.33a}$$

where γ_α and γ_s are the surface free energies of the adhesive and substrate and γ_{as} is the interfacial free energy. In the presence of a liquid such as water, this equation must be modified for the free energies with a physically absorbed surface layer:

$$W_{Al} = \gamma_{al} + \gamma_{sl} - \gamma_{as} \tag{9.33b}$$

where γ_{al} and γ_{sl} are, respectively, the interfacial free energy between adhesive/liquid and substrate/liquid.

In air W_A is generally positive, indicating thermodynamic stability of the bond. However, in water W_{AL} can be negative, indicating that the bond is unstable; it can be displaced by moisture. For the aluminum-oxide/epoxy-adhesive bond,[33] $W_A = 291$ mJ m^{-2} whereas in water $W_{AL} = -137$ mJ m^{-2}, indicating instability. In contrast, for the carbon/epoxy-epoxy bond, $W_A = 88$–99 mJ m^{-2} and $W_{AL} = 22$–44 mJ m^{-2}, indicating stability.

The case of chemical stability of the surface is much more complex to analyze. The stability of bonds to metals depends critically on the type of oxide produced by the surface treatment procedure. In the case of aluminum, some types of oxide are hydrated in a moist environment with catastrophic loss in bond strength. For attack to occur (in the absence of disbonds, etc.), the moisture level in the adhesive needs to reach a critical level; for the case of epoxy bonds to steel, this (as mentioned previously) was found to be about 1.4%.

Unless fairly elaborate surface treatment procedures and primers are used, metal bonds to epoxy adhesives are prone to degradation in humid environments, whereas similar bonds to epoxy-matrix composites appear to pose no durability problems, even with very simple abrasive surface treatments.

9.3.14 Treatment of Composite Surfaces for Bonding

A common factory approach for bonding precured composite adherends relies on the use of a peel ply, which is a layer of woven nylon cloth incorporated into the surface of the composite during manufacture. Before bonding, the nylon is peeled off, exposing a clean surface ready for bonding. However, it is generally considered that such bonds are inferior to those effected by grit blasting because the grid-like nature of the peeled surfaces encourages air entrapment; there is also the significant danger of small amounts of the peel ply[35,36] or, where used, silicone release agents transferring as a thin layer to the bonding surface.

For thermosetting-matrix composites, the most effective surface treatment for strong durable bonding is to grit-blast with alumina or silicon carbide particles.[37] When done correctly, this process provides a clean, uniform, high-energy surface.

Thorough abrasion of the surfaces with silicon-carbide paper or abrasive pad is a reasonable alternative,[38] but is less satisfactory because minor depressions in the surface are left untreated unless a considerable amount of surface material is removed. This will result in a weaker joint as areas of unbraided surface resin will remain. Because the surface resin on the composite has a much lower fracture energy than that of the adhesive, there is merit in removing all or most of this layer.

In contrast with thermosets, thermoplastic-matrix composites, because of the low surface energy, require aggressive chemical surface treatments to form strong bonds with thermosetting adhesives.[39] Methods based on chemical or plasma discharge etching have proved reasonably successful[40] but the bonds formed are generally weaker than those made to a thermosetting-matrix composite. Thermoplastic films with a lower melting point than the matrix polymer may be a better option. For example, PEI film can be used to join (or more likely repair) PEEK matrix composites.[41]

9.4 Mechanically Fastened Joints

Symbols

Allowable materials strength in tension	σ_{tu}	Elastic tensile stress concentration factor in infinitely wide plate with unloaded hole	K_t
Allowable far-field tensile stress	σ_u	Elastic isotropic tensile stress concentration factor, with respect to net tension stress	K_{te}
Allowable far-field tensile strain	ε_u	Effective tensile stress, with respect to net tension stress	K_{tc}
Allowable materials strength in shear	τ_u	Effective tensile stress concentration factor for loaded hole, with respect to hole diameter	K_{tbc}
Through-thickness stress	σ_z	Load capacity of joint per unit width	P
Allowable materials strength in bearing	σ_{bgu}	Load on joint per unit width	p
Tensile stress bypassing hole	σ_{by}	Correlation coefficient between experimental and observed stress concentration factors	C
Bearing stress	σ_{bg}	Hole or fastener diameter	d
Modulus in load direction	E_x	Strip width	w
Modulus normal to load direction	E_y	Strip thickness	t
Shear modulus, in plane	G_{xy}	Edge distance	e
Major Poisson ratio	v_{xy}	Stress ratio, minimum/maximum	R
		Torque	T

9.4.1 Introduction

This section describes simple design procedures and materials engineering topics relevant to the application of mechanical joints in composite airframe structures.

Intuitively, it may be concluded that mechanical fastening is an unsatisfactory means of joining composites because the fastener holes must cut fibers, destroying part of the load path. However, although considerable loss in strength occurs (typically to half of the original strength), acceptable joints can be made. Indeed, mechanical fastening is usually the only feasible or economic means of joining highly loaded (thick) composite components.

9.4.1.1 General Design Considerations. Although the aim of achieving smooth load transfer from one joint element to another is similar in bonding and mechanical fastening, the load transfer mechanisms are very different.

In mechanical fastening, load transfer is accomplished by compression (bearing) on the faces of holes passing through the joint members by shear (and, less desirably, bending) of the fasteners.

Some of the load is also transferred through friction on the face of the joint element if the clamping forces imposed by the fasteners is sufficient. However, although high clamping forces (bolt-tightening torque T) are very important to develop high-friction forces to maximize bearing strength, it may not be possible to maintain these levels of clamping force during prolonged service, for example, due to wear under service loading conditions.

Because high through-thickness reinforcement is provided by the fasteners, peel failure of the composite is generally not a problem. However, problems can arise resulting from the relatively low bearing and transverse strengths of the composite compared with those of metals. Bearing failure results in hole elongation, allowing bending and subsequent fatigue of the bolt or substructure. Alternatively, the fastener head may pull through the composite.

Figure 9.23 illustrates the failure modes of a composite joint.[42] In tension, the main modes are tension failure of the net section, bearing, and shear failure.

In addition (Fig. 9.23), mixed-mode failures can occur, including cleavage tension, essentially mixed tension/shear; bolt-head pulling through the laminate, a problem particularly with deeply countersunk holes; and bolt failure due to bearing failure.

The type of failure that occurs depends on the ratio of the effective width to the diameter of the fastener hole w/d, and the ratio of the edge distance to the diameter e/d. The variation of failure load with w/d and e/d for a quasi isotropic laminate is indicated in Figure 9.24. For large w/d and e/d, the joint fails in

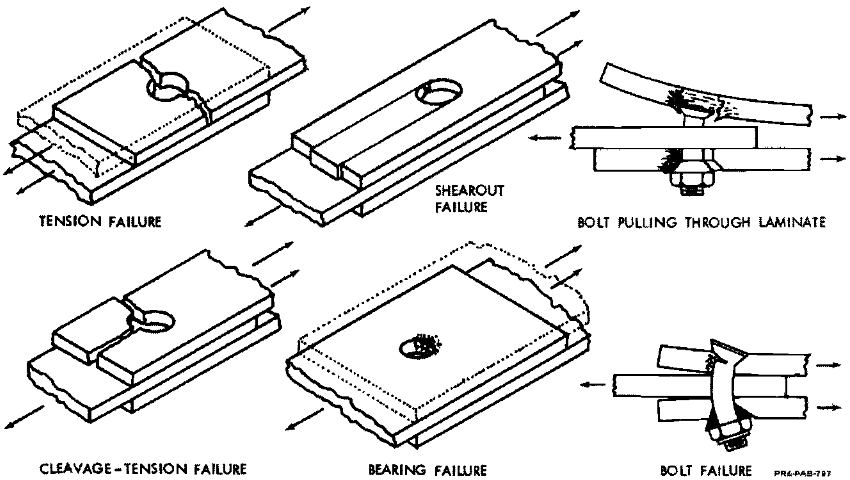

Fig. 9.23 Schematic illustration of the main failure modes in mechanical joints in composites. Taken from Ref. 42.

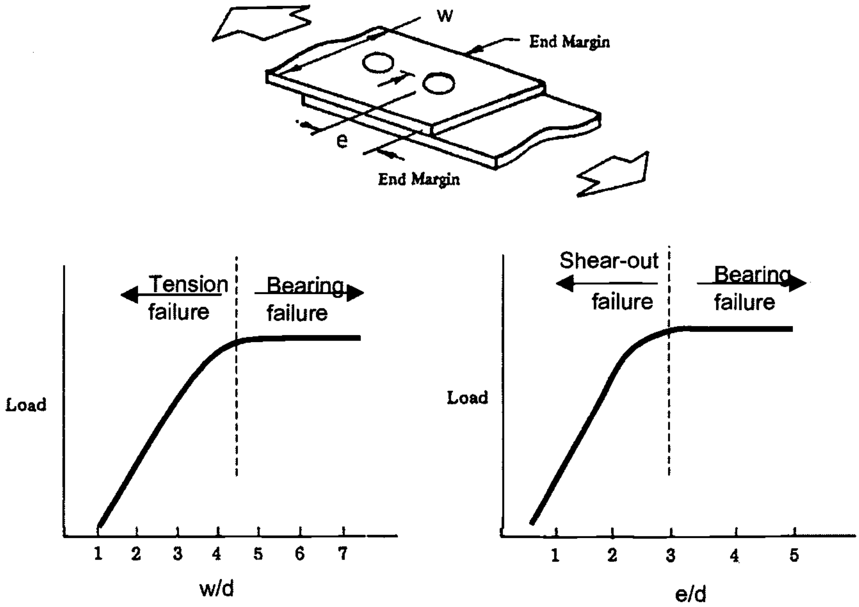

Fig. 9.24 Transition between failure modes with specimen width (rivet pitch) and edge distance.

bearing, and the failure load is independent of w/d or e/d. With reduced w/d tension failure of the net section will occur with the joint strength dropping to zero when $w/d = 1$. If the edge distance e is reduced, shear failure occurs with the strength of the joint dropping to zero when $e/d = 0.5$.

The allowable stresses in each of these modes is a function of:

- Geometry of the joint, including thickness
- Hole size, spacing, and bearing area, allowing for countersink
- Fastener loading, single or double shear; that is, loading symmetrical, as in a double-lap joint, or unsymmetrical, as in a single-lap joint
- Fastener fit tolerance
- Clamping area and pressure, allowing for any countersink
- Fiber orientation and ply sequence
- Moisture content and service temperature
- Nature of stressing: tension, compression, shear; cyclic variation of stressing; any secondary bending, resulting in out-of-plane loading. Stresses due to thermal expansion mismatch in metal-to-composite joints may also have an effect, but these are rarely considered in mechanical joints

The ply configuration in most bolted joints is usually chosen to be close to quasi isotropic, based on 0°, ± 45°, and 90° fibers. The non-zero fibers are needed to carry load around the hole to prevent shear or cleavage-type failures, whereas the 0° fibers carry the primary bearing loads and tension. The desired failure mode is usually net tension or compression; however, in some situations (the softer or less catastrophic) bearing failure may be preferred.

If stiff (highly orthotropic) laminates are required for a particular application, a higher proportion of 0° fibers may be used and further measures, discussed later, may be required to increase hole strength.

9.4.2 Design Criteria for Failure of Single-Hole Joints Under Static Tensile Loads

9.4.2.1 Stress Concentrations in Laminates with Unloaded Holes. It is instructive to consider the elastic stress concentration factor K_t for an unloaded hole in an infinite plate because this case has been solved analytically.[43] This situation is relevant to joints having significant bypass loads, as described later.

The analysis gives the effective K_t at the edge of the hole at 90° to an applied tension stress as:

$$K_t = 1 + \sqrt{\left\{2\left[\sqrt{\left(\frac{E_x}{E_y}\right)} - \gamma_{xy}\right] + \frac{E_x}{G_{xy}}\right\}} \tag{9.34}$$

It is shown that K_t at the edge of the hole, at 90° to the applied load, varies from 7.5 for a 100% 0° laminate to about 1.8 for a 100% ± 45° laminate and approaches the isotropic value of 3.0 at 80% ± 45°. Because the tensile strength falls with increasing ± 45°, it can be shown that the optimum ply configuration is about 50% ± 45°.

Actually, the peak stresses do not necessarily occur at 90° to the applied load. For example, in the case of an all ± 45° laminate, it occurs at 45° to the loading direction.

Stresses in the individual plies vary with their orientation and are complex involving in-plane and through-thickness components. It is thus difficult to develop suitable failure criteria, particularly because some of the failure modes, such as local splitting and delamination, are highly beneficial in reducing the peak stresses. Failure of the laminate is generally considered to have occurred (analytically) when the load is sufficient to cause fiber failure in one of the plies, based on criteria for complex loading, such as Tsai-Hill (see Chapter 6).

There are several semi-empirical methods of assessing the tensile strength of composite panels with unloaded holes of finite width. The main approaches[44] used are:

- Average stress criterion: Failure is considered to occur when the *average* value of the tensile stress over some characteristic length a_o from the hole reaches the unnotched failure strength σ_{tu} of the laminate.

- Point stress criterion: Failure is considered to occur when the *local* value of stress at some characteristic distance d_o from the hole reaches the unnotched failure strength σ_{tu}.

The values of a_o or d_o, considered to be materials properties, are determined from plots of strength reduction versus hole size to give the best fit to the experimental results. These criteria are related, through $a_o = 4d_o$.

Unfortunately, there are problems with these approaches; for example, they usually do not predict the actual locus of failure. However, the approaches are used extensively in the aerospace industry with some success and have been applied to more complex problems, including bi-axial and compressive loading of unloaded holes and to stresses arising from bearing loads.[45,46]

In the following sections, the tensile load capacity P is estimated for each of the main failure modes in a simple joint, such as shown in Figure 9.25. The more complex behavior in compression loading, non-symmetrical loading, or in multi-hole joints will be considered later.

The approach taken here is largely based on that developed by Hart-Smith and reported in several papers and reports, the most detailed being Ref. 42.

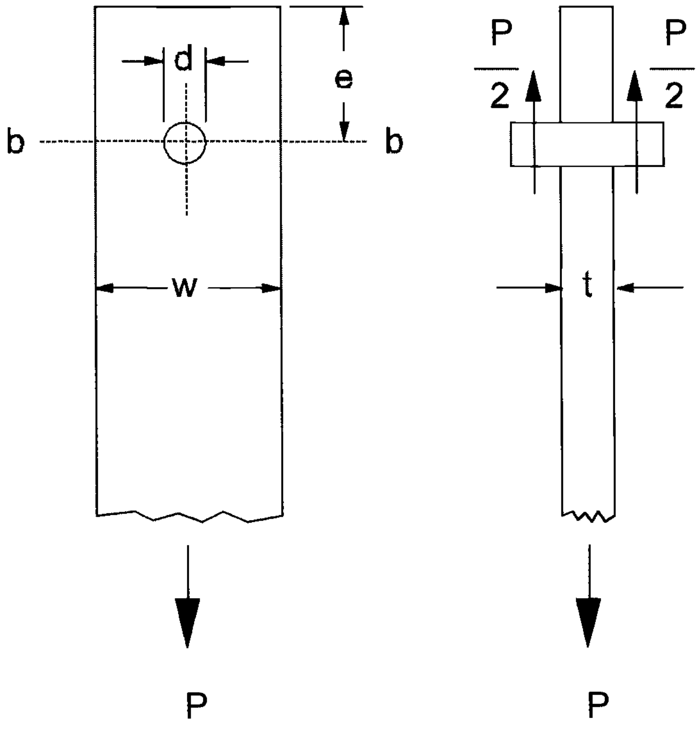

Fig. 9.25 Geometry of a simple double-lap bolted joint used to obtain test data.

9.4.2.2 Tension Failure. The maximum tensile stress $\sigma_{\max}$ at the edges of a loaded hole in a joint under an arbitrary load P, such as shown in Figure 9.25, is given by:

$$\sigma_{\max} = \frac{K_{tc}P}{t(w-d)} \tag{9.35}$$

where K_{tc} is the *effective* stress concentration factor, based on net section.

Thus, the joint strength efficiency, expressed as the ratio of (load capacity of the joint, P)/(unholed load capacity), is given by:

$$\frac{\sigma_u}{\sigma_{tu}} = \frac{P}{\sigma_{tu}wt} = \frac{(1-(d/w))}{K_{tc}} \tag{9.36}$$

For metals at high stresses, the effective stress concentration factor $K_{tc} \approx 1$ because, as discussed previously, yielding reduces the elastic stress concentration so that the failure strength is simply dependent on net sectional area, whereas for a brittle material (or for the metal at stresses below yield) $K_{tc} = K_{te}$. For the composite, K_{tc} will fall somewhere between these two extremes with microcracking of a brittle matrix locally softening the material in the vicinity of a stress concentration.

Based on the early experimental work of others for an elastic isotropic joint element (having a large edge distance e), Hart-Smith[42] recommends the following empirical relationship for the elastic stress concentration:

$$K_{te} = \frac{w}{d} + 1 - 1.5\frac{(w/d-1)}{(w/d+1)} \tag{9.37}$$

Thus, for $d/w = 0.1$, $K_{te} \approx 10$ while for $d/w = 0.33$, $K_{te} \approx 3.3$, showing the large stress concentration associated with bearing loads acting on a small hole.

For an elastic isotropic material, using equations (*9.35*) and (*9.36*), the ratio joint strength/basic strength is given by:

$$\frac{P}{\sigma_{tu}tw} = \frac{1}{2/(1-d/w) + 1/(d/w) - 1.5/(1+d/w)} \tag{9.38}$$

This relationship is plotted in Figure 9.26 and shows that the peak strength of the joint is about 20% of nominal tensile strength at a d/w of about 0.4.

To allow for stress reduction in composites at failure loads, the relationship between K_{tc} and K_{te} is determined experimentally from strength tests on joints (as shown in Fig. 9.25), equation (*9.36*) is used to find K_{tc} and equation (*9.37*) to estimate K_{te}. An approximate linear relationship is found. Because the two coefficients must be equal at $K_{te} = 1$, the equation used is:

$$K_{tc} - 1 = C(K_{te} + 1) \tag{9.39}$$

where C is the correlation coefficient for the particular laminate, environmental conditions, and geometry of the joint. A value of $C = 0$ indicates full relief of the

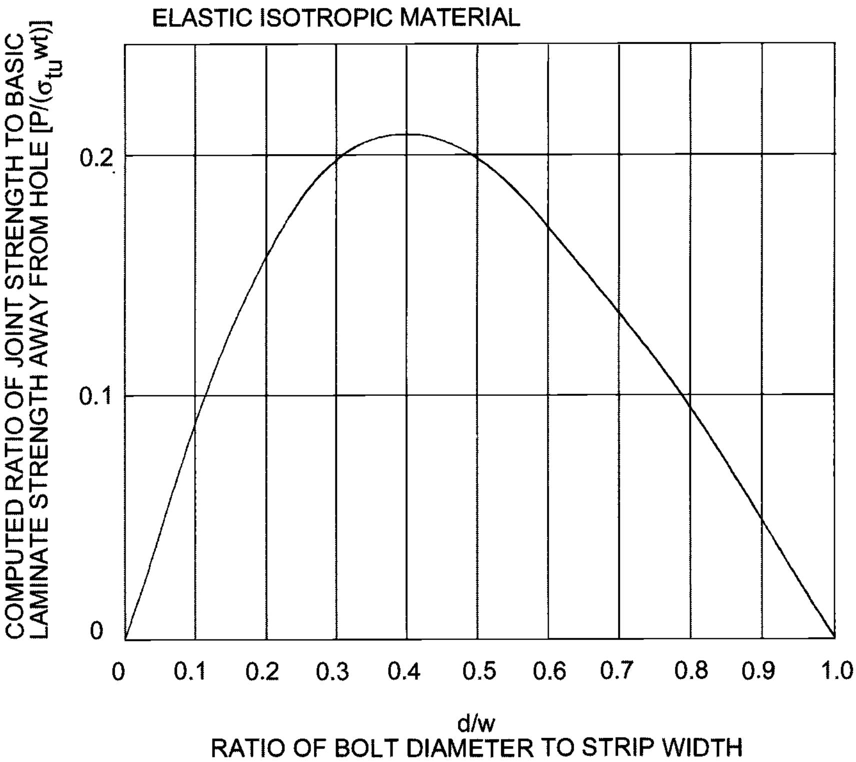

Fig. 9.26 Plot of ratio of joint strength to basic laminate strength versus d/w for an elastic isotropic material, assuming net tension failure. Based on Ref. 42.

stress concentration, whereas $C = 1$ indicates a brittle material where equation (*9.38*) applies.

For composites, C depends on fiber pattern and hole size and probably on temperature and moisture content in the laminate. For a first generation quasi isotropic composite, C was found to be around 0.25 for a standard 6.35-mm bolt hole; coincidentally, this is numerically similar to the fraction of 0° plies used in the experiments; although for a more highly anisotropic composite, C can range up to 0.5.

A comprehensive study[47] of the loaded hole strength of laminates based on carbon/epoxy cloth with a $[0°/45°]_{2s}$ lay-up provided the values for C listed in Table 9.5. This shows that the laminate becomes significantly more notch-sensitive at 180 °C. This is thought to be associated with the marked softening (effective toughening) of the matrix at elevated temperature, inhibiting the formation of delaminations around the hole. The effective stress concentration K_{tc} then becomes closer to the elastic value, Table 9.5, favoring fiber failure rather than delamination, and resulting in significant strength reduction. Similar behavior may be expected with thermoplastic-matrix composites (and even

Table 9.5 Data from Tensile Tests on Loaded Holes in [0°/45°]$_{2s}$ Carbon/Epoxy Cloth Laminates; the Bolt Size was 4.76 mm, d/w = 0.375, and the Computed K_{te} is 3.0

Temperature, °C	K_{tc}	C
24	1.36	0.18
120	1.33	0.18
180	1.71	0.36

highly toughened epoxies), even at ambient temperature, because these composites are highly resistant to delamination.

9.4.2.3 Bearing Failure. The bearing capacity P of a joint, such as shown in Figure 9.25, involving metallic adherends, is generally based on the nominal bearing strength σ_{bgu} using the relationship:

$$P = \sigma_{brgu} dt \tag{9.40a}$$

Thus, the joint efficiency ratio for bearing failure is given by:

$$\frac{P}{\sigma_{bgu} wt} = \frac{d}{w} \tag{9.40b}$$

In carbon/epoxy composites, failure in bearing occurs by local buckling and kinking of the fibers and subsequent crushing of the matrix.[48] The compressive stress to predict microbuckling of the fibers is given by equation (2.28). Consequently, the bearing strength σ_{bgu}, and thus the load carrying capacity P, are strongly dependent on the degree of constraint (clamping stress σ_z) provided by the fastener and on the properties of the matrix.

Experimental studies[49] on the influence of clamping pressure σ_z on ultimate bearing strength σ_{bgu} (Fig. 9.27), show that an improvement in bearing load of 60–170% can be obtained over pin loading with σ_z up to around 20 MPa; above this pressure, little further improvement is obtained. A typical value for the optimum σ_{bgu} is about 1000 MPa.

The clamping pressure in these plots was estimated from:

$$\sigma_z = 1.658 \frac{T}{d^3} \tag{9.41}$$

based on the clamping area with a standard washer, taking the diameter of the washer to be 2.2d and assuming a torque stiffness coefficient of 0.2.

There is also some load transfer simply due to friction between the fastener or washer and joint element. Tests[50] were undertaken to measure the *effective* bearing strength with 1) simple pin loading, 2) clamp up (no bolt), and 3) a standard bolt under moderate torque. Figure 9.28 plots the experimental results, showing that friction makes a significant contribution to bearing strength.

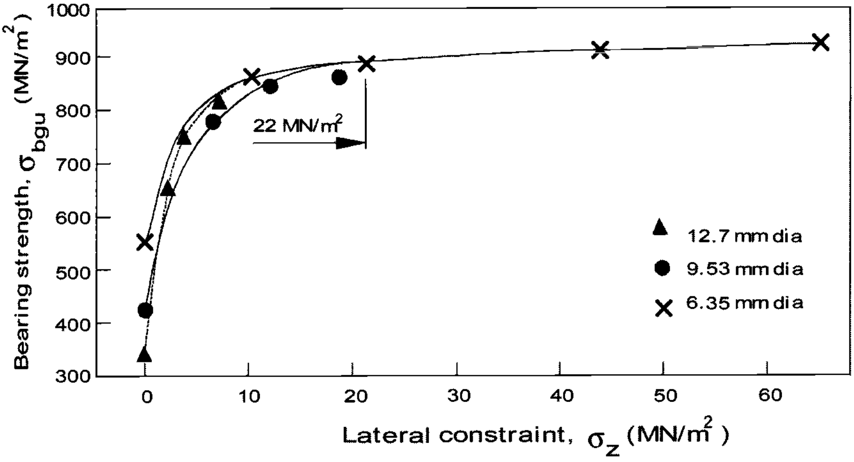

Fig. 9.27 Bearing strength versus clamp-up pressure for a 0°, ±45° 12-ply laminate with various hole sizes. Taken from Ref. 49.

Because clamping plays such an important role in the bearing strength of composites, it is important to ensure that this pressure is maintained under service conditions.

Bearing strength initially increases with increasing proportions of 0° plies because these are the most efficient in carrying the bearing loads. However, once the proportion of 0° plies exceeds about 60%, failure occurs by splitting because the transverse strength then becomes insufficient to prevent shear failure, even at very large values of e, the edge distance. The optimum bearing strength for a 0°/±45° laminate occurs at about 50% 0° and 50% ±45° plies. It is found that the bearing strength is further improved as the ply sequence is made more homogeneous (dispersion of 0° and ±45° plies). As is well known, interply stresses are reduced as the laminate becomes more homogeneous.

Although the compressive strength of the composite undergoes significant reduction at elevated temperature, particularly under hot/wet conditions, loss in bearing strength in joints can be reduced by maintaining high local constraint through bolt clamping. Furthermore, matrix softening may reduce local high loads through better contact of the fastener with the hole. Figure 9.29 shows that reasonable bearing strength for two extensively used (180 °C—curing) composite systems[47] is maintained well above 120 °C.

9.4.2.4 Shear-Out Failure. For metallic adherends, load-carrying capacity in shear is usually estimated from the following simple relationship:

$$P = \tau_u 2et \tag{9.42}$$

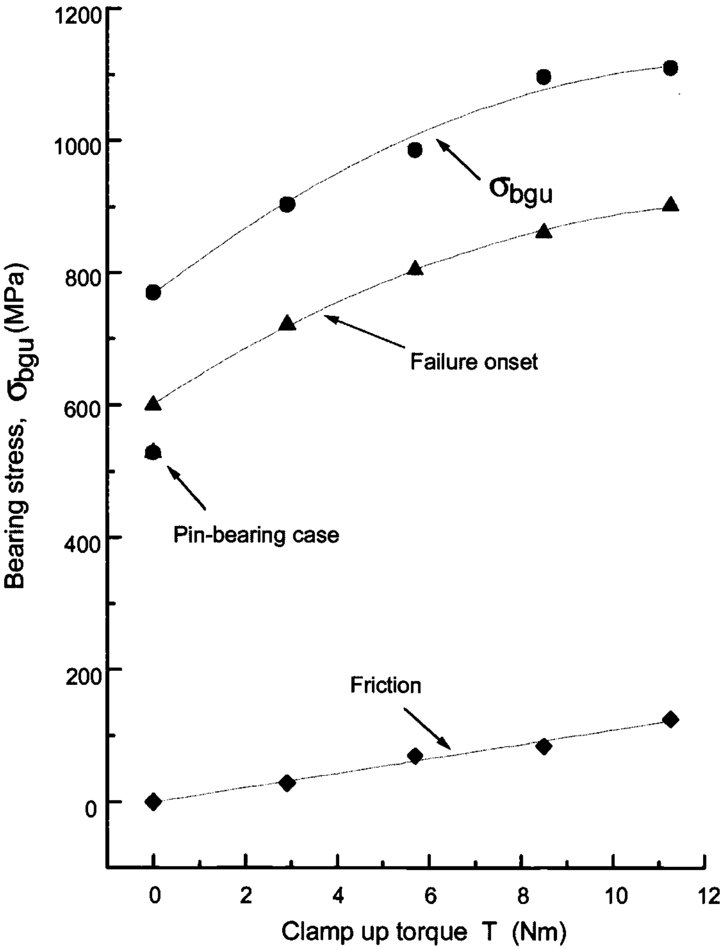

Fig. 9.28 Static strength versus torque for a single-hole joint fastened with 6.35-mm bolt or pin. Taken from Ref. 50.

Experimental results indicate that this relationship holds reasonably well for carbon/epoxy composites providing there are about 50% $\pm 45^\circ$ plies, implying that there is little stress concentration for this loading condition. To ensure that the joint strength is not limited by either net-tension or shear-out strength (with laminates containing sufficient percentages of $\pm 45^\circ$ plies) a minimum w/d of about 5 and an e/d ratio of about 3 are required.

In contrast, significant stress concentrations occur with high percentages of 0° plies because the apparent τ_u falls well below the value measured by standard shear tests. In fact, under these conditions, failure occurs by splitting rather than by shear (or bearing), and strength is unaffected by the shear distance e.

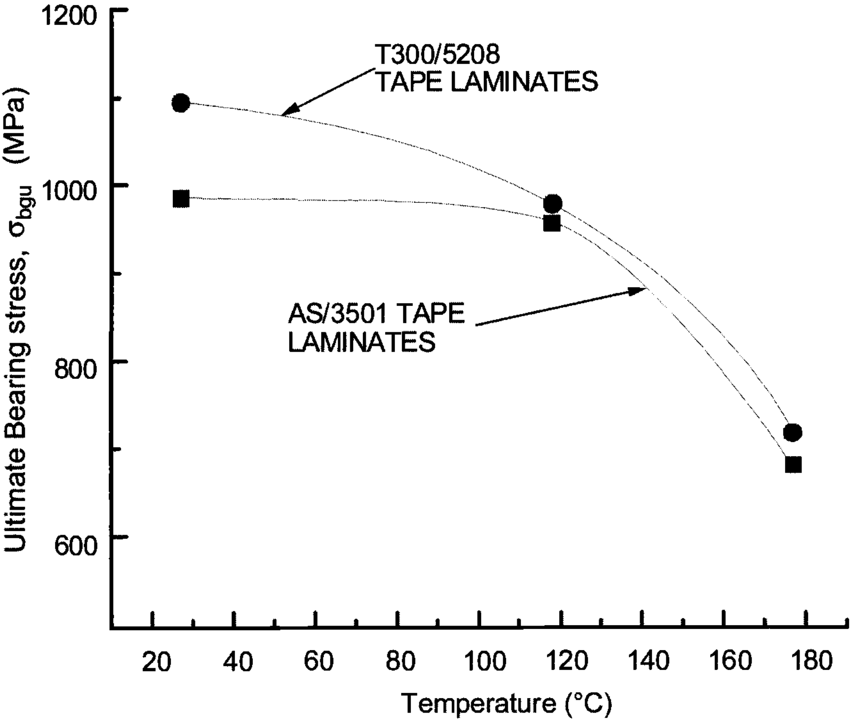

Fig. 9.29 Bearing strength as a function of temperature for two carbon/epoxy composite systems. Taken from Ref. 47.

9.4.3 Single Fastener Joint Loading Efficiency in Tension

The conclusion from the above consideration of failure modes for a single-hole joint is that a quasi isotropic laminate with well-dispersed plies provides the optimum strength in mechanical joints. Assuming that the joint is designed to avoid the shear and cleavage failures shown in Figure 9.23 by having appropriate ply configuration and an e/d of at least 3, only net-section tension and bearing failures need be considered.

Figure 9.30, taken from Ref. 42, plots $P/\sigma_{tu}wt$, the joint strength efficiency, versus d/w for the metal, brittle material (using equation (*9.38*), and composite (assuming $C = 0.25$). The cut-off in net-section strength for bearing failure is shown only for the metal and composite. For the brittle material, it is seen that a maximum strength of 21% of the strength of the virgin material is reached at $d/w = 0.4$.

In the case of both the metal and the composite, a change in failure mode from net-tension to bearing is predicted to occur at d/w of approximately 0.3. The net-tension/strength plot for the metal results from using equation (*9.36*) for P/σ_{tu}, taking $K_{tc} = 1$ with an appropriate value for σ_{tu}. The bearing strength plot results from using equation (*9.40b*) with an appropriate value for σ_{bgu}.

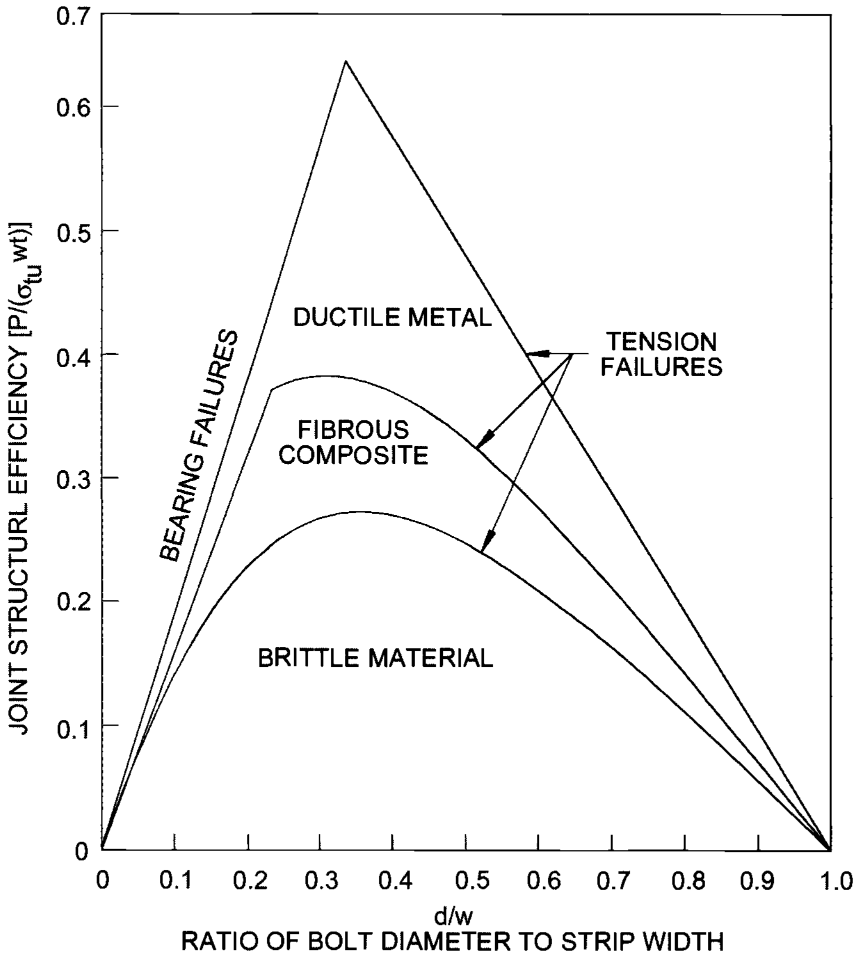

Fig. 9.30 Joint efficiency versus d/w for single fastener joints based on metal, composite, or brittle components under tensile loading. Only bearing or net tension strengths are considered. Taken from Ref. 42.

For estimating the net tension strength of the composite, equation (*9.36*) is used with equations (*9.37*) and (*9.39*) for K_{tc}, with an appropriate value for σ_{tu}, whereas for bearing strength equation (*9.40b*) is used with an appropriate value for σ_{bgu}.

For the composite, the maximum strength efficiency is only about 40%, whereas for the metal it is about 65%.

9.4.4 Single Fastener Joint Loading Efficiency in Compression

Compression strength is significantly higher than tension strength for a loaded hole because some of the compression load can be transmitted directly through the fastener. The degree to which this can occur is dependent on the fit of the fastener in the hole. For a fastener with large clearance, the stress concentration will be similar to that experienced under tension, although the actual failure mode would be quite different. Typical hole clearance for fasteners in composites range from 0.1 mm to zero for interference fit.

9.4.5 Multi-Row Joints

The main objective of using multi-row joints is to minimize the peak bearing load, avoiding the cut-off due to bearing failure shown in Figure 9.30. However, to achieve improved strength, the joint has to be designed to ensure even load sharing between the fasteners. An analysis for load distribution for a joint with three rows of fasteners is outlined in Figure 9.31, and the outcome is illustrated in Figure 9.32. Figure 9.33 illustrates, schematically, the comparison in load distribution between a multi-row metallic joint in which the elements are able to yield and a typical composite joint[51] with no yielding or softening. Computer programs have been developed to execute this elastic analysis.[56,57] Data is required for in situ flexibility of fasteners. If the joint has been correctly designed to reduce bearing loads, failure under tensile loading will occur in net tension. However, there are now two sources of tensile stress at the edge of the fastener hole:

Caused by the load reacting out on the fastener by bearing
Caused by the load bypassing the fastener to be reacted out on other fasteners along the joint

The experimental approach to finding the allowable load on a composite joint is to produce a plot, such as in Figure 9.34, in which the outer envelope of allowable gross strain ε_u (away from the fastener hole) is shown as a function of the bearing stress σ_{bg}. All that is then needed is to establish, by analysis, the peak bearing stress in the critical hole in the joint. In Figure 9.34 the allowable gross strain for pure bypass was established as 4000 microstrain, reducing to 3000 microstrain at the bearing stress cut-off at $\sigma_{bgu} = 690$ MPa for the configuration under examination.

These envelope plots can be produced by measuring 1) the failure strain of a joint element $3d$ or $4d$ wide with an *unloaded* fastener hole that should fail in tension at the fastener hole, 2) the bearing stress σ_{bgu} in a much wider strip (typically $6d$) forced to fail in bearing, and 3) the failure strain of a $3d$ or $4d$ wide specimen designed to fail in tension at the hole at some combinations of bypass and bearing.

A more sophisticated approach is described in Ref. 52 using a mechanical test machine based on two independent servo-loading systems. One servo loads the joint element while the other loads the bolt hole by directly applying load to the bolt.

Figure 9.35 shows (a simplified version of) the envelope obtained[52] under tension or compression bypass loading. The plot shows the results for the onset of

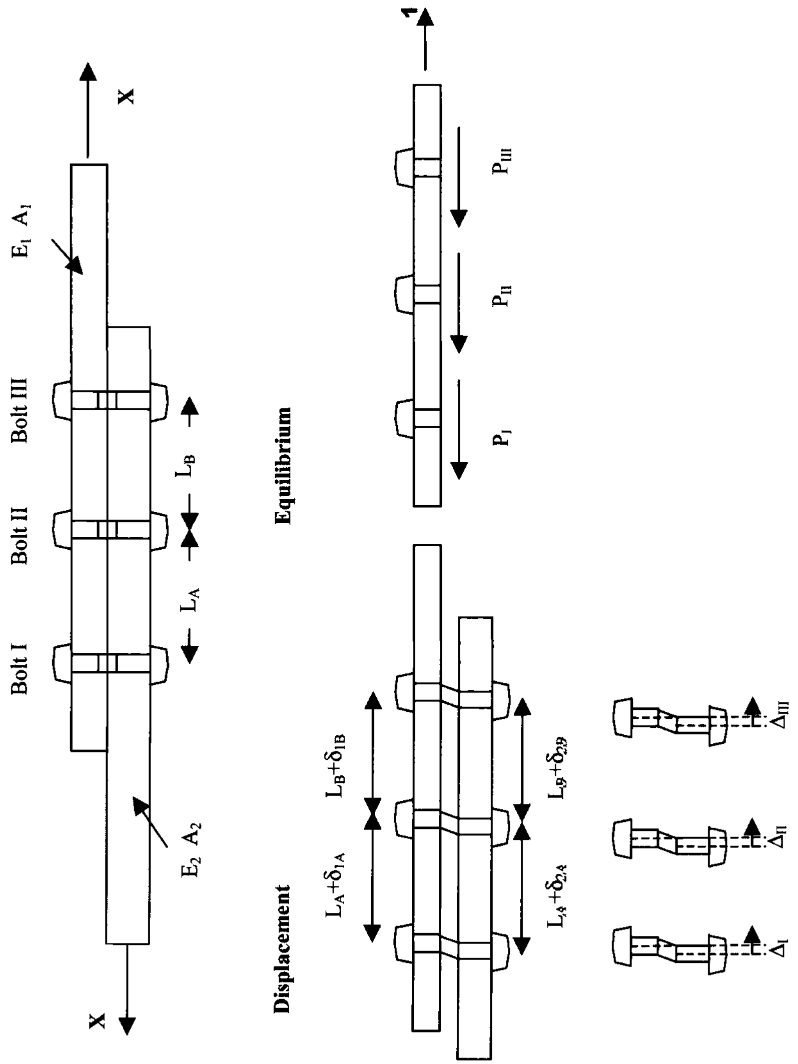

Bolt I
Bolt II
Bolt III
E_1 A_1
E_2 A_2
X
X
L_A
L_B
Equilibrium
Displacement
P_I
P_{II}
P_{III}
1
$L_A+\delta_{1A}$
$L_B+\delta_{1B}$
$L_A+\delta_{2A}$
$L_B+\delta_{2B}$
Δ_I
Δ_{II}
Δ_{III}

Compatibility

$$\delta_{2A} - \delta_{1A} = \Delta_{II} - \Delta_{I}$$

$$\therefore \delta_{1A} - \delta_{2A} + \Delta_{II} - \Delta_{I} = 0$$

$$\therefore \delta_{1B} - \delta_{2B} + \Delta_{III} - \Delta_{II} = 0$$

Equilibrium

$$P_I + P_{II} + P_{III} = X$$

Material

$$\delta_{1A} = \frac{L_A}{E_1 A_1} P_I \qquad \delta_{2A} = \frac{L_A}{E_2 A_2}(X - P_I)$$

$$\delta_{1B} = \frac{L_B}{E_1 A_1}(P_I + P_{II}) \quad \delta_{2B} = \frac{L_B}{E_2 A_2}(X - P_I - P_{II})$$

$$\Delta_I = P_I f_I$$

$$\Delta_{II} = P_{II} f_{II}$$

$$\Delta_{III} = P_{III} f_{III}$$

Hence

$$P_I + P_{II} + P_{III} = X$$

$$-\frac{L_A}{E_1 A_1} P_I + \frac{L_A}{E_2 A_2}(X - P_I) + P_{II} f_{II} - P_I f_I = 0$$

$$-\frac{L_B}{E_1 A_1}(P_I + P_{II}) + \frac{L_B}{E_2 A_2}(X - P_I - P_{II}) + P_{III} f_{III} - P_{II} f_{II} = 0$$

Fig. 9.31 Model and analysis of the joint with multiple rows of fasteners; *f* is fastener flexibility.

Joint design	Controlling property	Simplified equations	Bolt loads
Fasteners very flexible (or plates able to yield in bearing—metals at ultimate load)	$f_I = f_{II} = f_{III}$ large	$P_I + P_{II} + P_{III} = X$ $P_{II} = P_I$ $P_{III} = P_{II}$	$P_I = X/3$ $P_{II} = X/3$ $P_{III} = X/3$ 
Balanced stiffness, fasteners very stiff (composite panels —elastic behavior)	$E_1A_1 = E_2A_2$. $f_I = f_{II} = f_{III}$ small	$P_I + P_{II} + P_{III} = X$ $P_I - (X - P_I) = 0$ $(P_I + P_{II}) - (X - P_I - P_{II}) = 0$	$P_I = X/2$ $P_{II} = 0$ $P_{III} = X/2$ 
Stiff fasteners — unbalanced joint 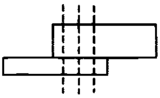	$E_1A_1 >> E_2A_2$. $f_I = f_{II} = f_{III}$ small	$P_I + P_{II} + P_{III} = X$ $(X - P_I) = 0$ $(X - P_I - P_{II}) = 0$	$P_I = X$ $P_{II} = 0$ $P_{III} = 0$ 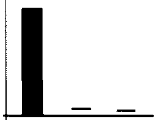
Stiff fasteners — unbalanced joint 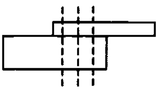	$E_1A_1 << E_2A_2$. $f_I = f_{II} = f_{III}$ small	$P_I + P_{II} + P_{III} = X$ $P_I = 0$ $P_I + P_{II} = 0$	$P_I = 0$ $P_{II} = 0$ $P_{III} = X$ 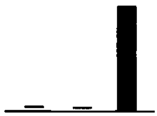

Fig. 9.32 Representative load distributions in a joint with three rows of fasteners.

damage, which is generally what is required for design purposes. Also noted are the various damage modes.

For tension loading, the conditions for onset of damage are similar to those shown schematically in Figure 9.34, indicating a cut-off of tension-reacted bearing strength (TRB) for net-tension (NT) failures as the magnitude of σ_{by}

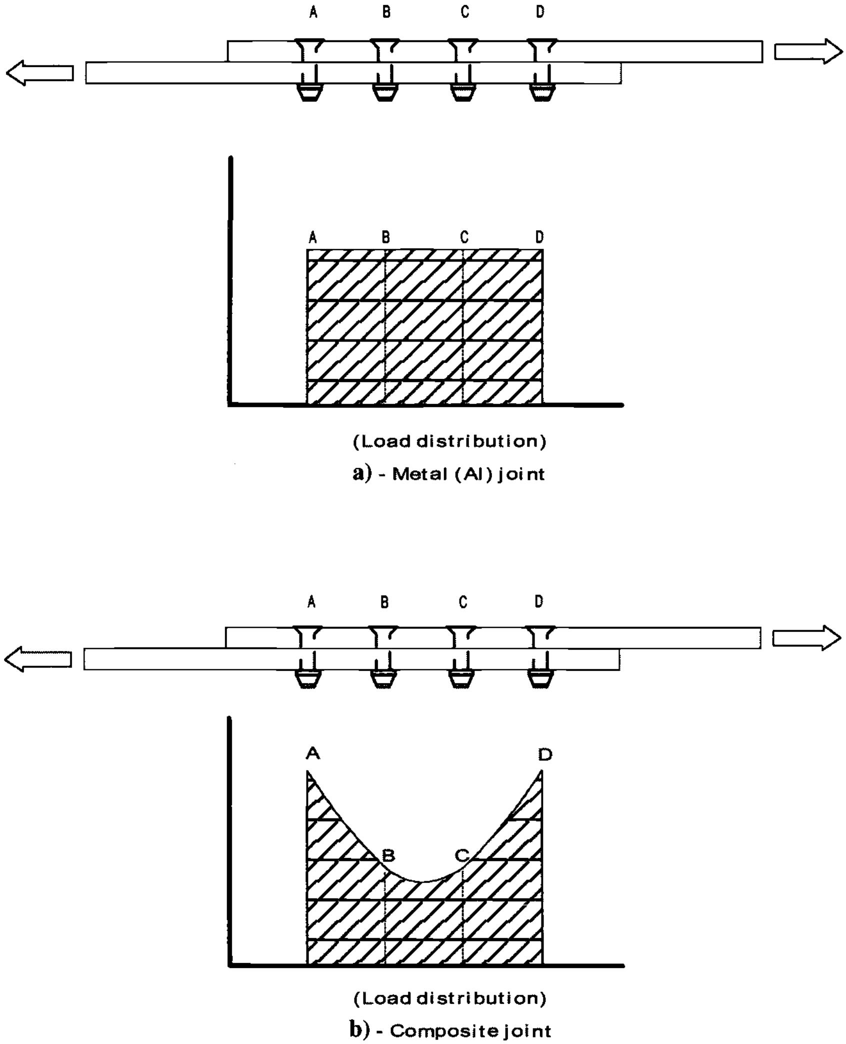

Fig. 9.33 Comparison of load transfer behavior, metals versus composites.

increases. The results are reasonably explained by the two straight-line plots, one for TRB failures and the other for NT failures.

Under compression loading, behavior is markedly different because the bolt (if clearances are small) can support the walls of the hole, transmitting part of the load directly and thus delaying the onset of net-compression (NC) failures. The predominant failure mode is thus compression-reacted bearing (CRB).

Hart-Smith[42] also developed an analytical approach for multi-row joints under tension in a strip width w, based on the hypothesis of linear interaction

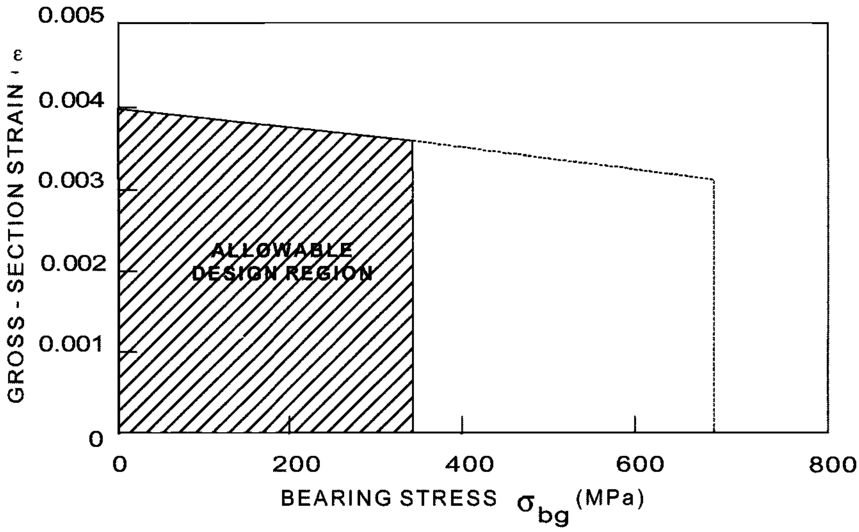

Fig. 9.34 Design allowables for bearing/bypass interaction under tensile loading.

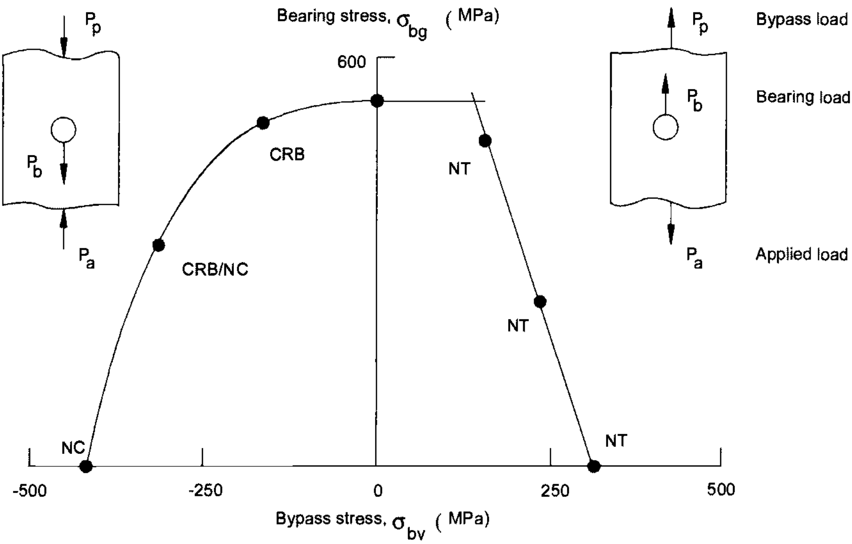

Fig. 9.35 Results of bearing/bypass experiments for tension or compression loading. Note failure in bearing (B), net tension (NT), net compression (NC), tension reacted bearing (TRB), and compression reacted bearing (CRB). Results are for a 16-ply quasi isotropic T300/5208 composite. Based on Ref. 52.

between the net-section bypass and bearing stresses, using the following relationship:

$$\sigma_{tu} = K_{tby}\sigma_{by} + K_{tb}\sigma_{brg}\ \left(\sigma_{brg} < \sigma_{brgu}\right) \tag{9.43}$$

The relationship for horizontal load equilibrium (at failure) is used to eliminate σ_{by}:

$$\sigma_{\max} = \sigma_{brg}\left(\frac{d}{w}\right) + \sigma_{by}\left(1 - \frac{d}{w}\right) \tag{9.44}$$

Thus:

$$\sigma_{\max} = \sigma_{brg}\left(\frac{d}{w}\right) + \left(1 - \frac{d}{w}\right)\left(\frac{\sigma_{tu} - K_{tb}}{K_{tby}}\right) \tag{9.45}$$

It is more useful to express these results in terms of allowable gross strain using:

$$\varepsilon_{tu} = \frac{\sigma_{\max}}{E_x} \tag{9.46}$$

The results can also be expressed in terms of gross-section structural efficiency for NT failure σ_{tu}/σ_u

Now the values of K_{tc} and K_{tbc} must be determined. Based on early work of others, it was shown that for the stresses associated with σ_{by}, the elastic stress concentration factor K_{te} for an *unloaded* hole in an isotropic strip width is given by:

$$K_{te} = 2 + (1 - d/w)^3 \tag{9.47a}$$

Thus, allowing for hole softening:

$$K_{tby} = 1 + C(K_t - 1) \tag{9.47b}$$

Because the tensile failure load P with no bypass can be expressed either in terms of net-section [equation (*9.35*)] or in terms of the contact area dt, we have that:

$$P = \sigma_{tu}\frac{(w - d)t}{K_{tc}} = \sigma_{tu}\frac{dt}{K_{tbc}} \tag{9.48a}$$

Thus,

$$K_{tb} = \frac{K_{tc}}{(w/d - 1)} \tag{9.48b}$$

Using equation (*9.45*) with equation (*9.46*) to obtain allowable strain and equations (*9.37*), (*9.39*), (*9.47*) and (*9.48*) for the K values, plots were developed such as in Figure 9.36 for the allowable strain (and structural efficiency) in multi-row joints. The figure plots the far field strain allowables at the most critical hole as a function d/w for various nominal values of bearing stress σ_{bg}. The values of σ_{bg} range from 0, for no bearing stress, to $\sigma_{bg} = \sigma_{bgu}$ where failure would occur in bearing. At all values of σ_{bg} below σ_{bgu}, failure occurs in NT.

The above relationships are also applicable for a wide joint element, having many columns of multiple fasteners spaced at d/w, using slightly modified values for the K constants.

Finally, for comparison, the relationships for a similar single-hole joint are also plotted in Figure 9.36 using the following equations.

Based on section strain away from hole,

$$P = \varepsilon_{tu} E_x wt \tag{9.49}$$

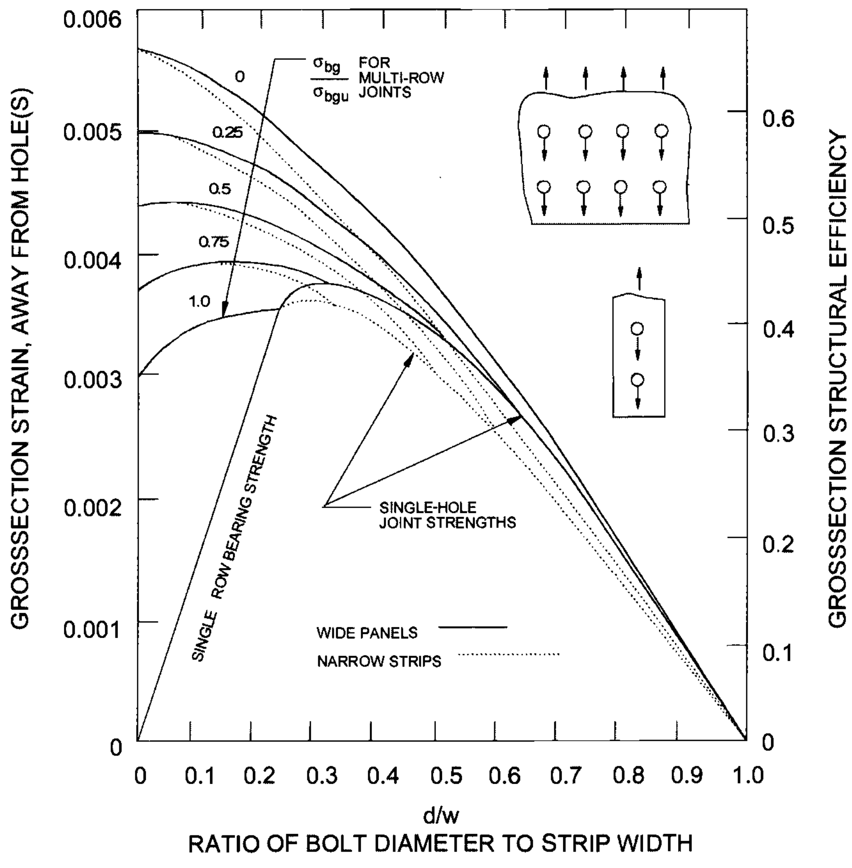

Fig. 9.36 Allowable strain and joint efficiency versus d/w for multi-row and single fastener composite joints under tensile loading. Only bearing or net-tension strengths are considered. Taken from Ref. 42.

Thus, for bearing,

$$\varepsilon_{tu} = \left(\frac{\sigma_{brgu}}{E_x}\right)\left(\frac{d}{w}\right) \tag{9.50}$$

and for NT failure,

$$\varepsilon_{tu} = \left(\frac{\sigma_{tu}}{E_x}\right)\left[\frac{(1 - d/w)}{K_{tc}}\right] \tag{9.51}$$

Figure 9.36 shows that:

- The maximum strength with multiple-row joints occurs when the bearing stress is zero, as expected. However, this is not a practical joint design, just the outer envelope of strength.
- At the optimum d/w ratio for a single-hole joint (approximately 0.3), the improvement with multi-row joints is not great for practical values of σ_{bg}. For example, for $\sigma_{bg}/\sigma_{bgu} = 0.5$, the improvement is only about 10%
- The only way of obtaining a major improvement over the single hole is to reduce d/w and also reduce bearing stresses by using joint designs that evenly share the bearing stress among several fasteners. This is difficult to achieve in practice and requires a very good design capability.

9.4.5.1 Optimum Design of Simple Multi-Row Joints. In most joint designs, it is desirable to modify the major components as little as possible for reasons of cost and repairability; it is much more efficient to modify the splice plate in the case of lap joints. The use of local build-ups or local inserts in the major components is very expensive, and therefore usually unacceptable, except where used for a single major attachment hole such as a lug. Furthermore, repair of a structure with modified holes may not be feasible because such modifications cannot be reproduced during repair.

The key to the optimization of load sharing in bolted joints using the procedures defined in Fig. 9.31 is in the modelling of effective fastener flexibility. This is expressed in terms of the sum of the following compliances[53]:

- Shear deformation of the bolt
- Bending deformation of the bolt
- Bearing deformation of the bolt
- Bearing deformation of the hole

Figure 9.37 is an idealized plot of load versus deflection[53] for a fastener in a simple joint such as shown in Figure 9.25. This shows deflection at zero or low load for take-up of clearance between the bolt and the hole (zero if interference fit), an initial line representing reversible elastic deflection and a line of a reduced gradient representing non-linear deflection due to hole elongation.

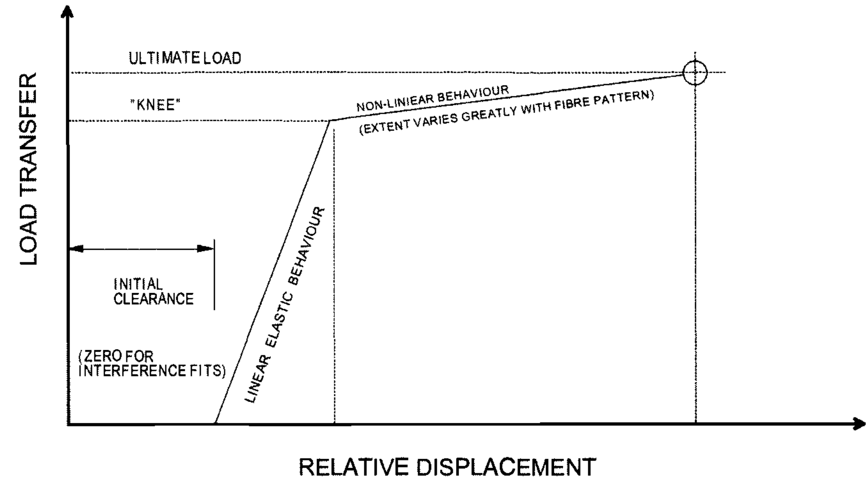

Fig. 9.37 Load versus deflection for a fastener, showing linear elastic region and non-linear region caused by hole elongation. Taken from Ref. 53.

Estimates can be made for the various compliances listed for the elastic region based on earlier studies on previous work on metallic joints.[53]

Using estimates of the compliances, based on earlier studies on metals, Hart-Smith produced the program (A4EJ), which allows estimation of load sharing between multiple fasteners.[56] Similar programs have been developed by the ESDU.[57]

An optimized design for a multi-row joint is shown in Figure 9.38. The approach (with reference to Fig. 9.36) involves use of tapered splice plates with various sized fasteners. The aim is to minimize the bearing stress in the inner (adjacent to the skin butt) fastener. Because in the skin this fastener has no bypass load, it is optimized as a single-hole joint with a d/w of 0.3 and a 15-mm bolt. The bypass and bearing loads in the splice plate are a maximum at this point. However, because the plate can be designed to be thick (more than half the equivalent thickness of the skin) at this point, with little weight penalty, it can

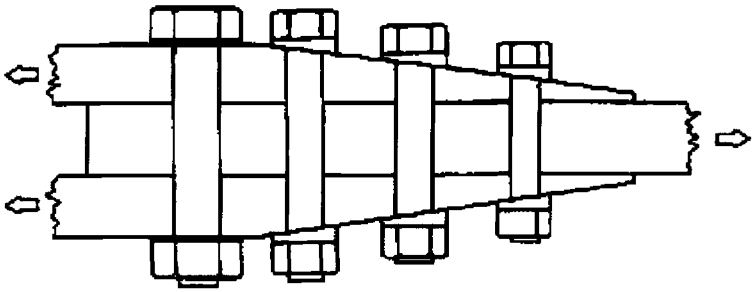

Fig. 9.38 Optimum design of multi-row lap joint. Taken from Ref. 53.

easily cope with these loads. The next two rows of fasteners have a smaller diameter with d/w of 0.25 because these experience some bypass load. The last (now critical) fastener, which has the maximum bypass load, is designed with a d/w of 0.2 to minimize bearing stresses (to 25% of σ_{bgu}). The gross strain allowable at this fastener, and consequently at the joint, is around 5000 microstrain, which is much higher than is possible with a single-hole joint.

9.4.6 Influence of Fatigue Loading

9.4.6.1 Open Holes. To understand the complex effects of cyclic loading on mechanically fastened joints, it is first helpful to appreciate degradation mechanisms in carbon/epoxy laminates with an unloaded hole. Under tension or compression-dominated loading,[54] failure initiates in the regions of high elastic stress concentration as matrix microcracking and local disbonding of fibers from the matrix. This damage significantly reduces the in-plane elastic stress concentrations thus *increasing* residual strength. The localized damage accumulates until it results in more extensive intralaminar cracking, eventually resulting in delaminations (separations between plies). The rate and extent of delamination formation depends on the magnitude of the interply peel and shear stresses, which are strongly dependent on the ply configuration. More homogeneous configurations (few groupings of plies having similar orientation) produce lower interply stresses.

From this stage, tension and compression behavior differ greatly. Under tension, the formation of the delaminations is generally beneficial because the damage is localized and generally does not propagate. Thus, for design purposes, it is usually necessary to consider only static strength, which is lowest before fatigue.

Under compression loading, although stress concentration at the edges of the hole is similarly reduced, the loss in section stiffness due to delaminations can lead to compression or buckling failure of the remaining sound material. Furthermore, the loss in laminate symmetry caused by the formation of delaminations produces interlaminar stresses that drive delamination growth and encourage instability. Compression fatigue strength similar to compressive static strength is degraded under hot/wet conditions.

It is of interest to compare this behavior with that of metals. Under relatively low cyclic stresses (below limit load for most of the life), the elastic stress concentrations at the edges of the hole are not relieved by gross plastic deformation. However, localized cyclic plastic deformation at the edge of the hole can occur at a relatively low stress (approximately one third limit load), leading to the initiation of fatigue cracks that can propagate predominantly under tensile components of the loading, eventually resulting in failure. Fatigue crack growth in metals usually cannot occur under pure compression loading. There is no equivalent to delamination growth, except under corrosive conditions in some aluminum alloys, in which exfoliation can occur in the material surrounding the hole.

9.4.6.2 Loaded holes. In loaded holes, superimposed on the behavior just described for the composite are (1) bearing stresses, which are detrimental, (2) lateral support and pressure from the fastener, which are beneficial, particularly in compression, and (3) support of the hole by the fastener in compression, also beneficial. Generally, a composite with a loaded hole in which fastener pressure can be maintained will have superior fatigue resistance to a similar composite having an open hole, even allowing for bearing stresses in the former case. However, if fastener pressure or fastener support is lost, due to partial bearing failure or wear, these benefits will be reduced or lost.

In practice, hole enlargement and a loss in residual strength are not serious problems in the allowable strain range if load reversal does not occur, and residual strength may increase after exposure to cyclic stresses with no stress reversal; e.g., for $R = -\infty$ (compression/zero) or $R = 0$ (zero/tension).

Fatigue tests conducted on joints (similar to that shown in Figure 9.25, with a 6.35-mm pin or bolt) under $R = 0.05$ (small-preload/tension) under dry and wet conditions[50] showed that with simple pin loading (i.e., no load carried by friction) little hole elongation occurred before fatigue failure, although fatigue failure occurred at a relatively low bearing stress. However, marked hole elongation (about 1 mm) occurred at a similar fatigue life at loads about 50% higher with $T \approx 0$ (hand tight) because the washers provided sufficient constraint to delay failure. At normal levels of T (around 6 Nm), fatigue strength was markedly improved and hole elongation at bearing failure greatly reduced. The effect of wet conditions at modest levels of T was to reduce the threshold level of stress for hole elongation, reducing the fatigue strength (based on a threshold level of hole elongation) by about 40%. This behavior was considered to be associated in part with a reduction in friction, due to the lubricating action of moisture, resulting in increased bearing stresses for a given T.

Loss in strength can be marked even at modest stress levels if stress reversal occurs, for example, $R = -1$ (equal tension and compression), even at reasonable levels of T. This is because, under this type of loading, gross fastener movement can occur, causing damage to both ends of the hole, resulting in extensive hole enlargement. The result is lack of fastener support under compression loading and, due to the relative movement, loss of clamping pressure. Furthermore, lack of support in the hole due to elongation leads to fastener pull-out or to fastener bending resulting in fastener fatigue failure. Movement of the fastener can also lead to fatigue cracking of the substructure, if this is metallic.

Frequent removal and replacement of fasteners[55] appears to accelerate the development of damage around the composite hole, resulting in a reduction in fastener fatigue life.

9.4.6.3 Problems with Single-Shear Joints and The Use of Countersinking. Double-shear joints, as shown in Figure 9.25 (similar to double-lap joints) are preferred because they usually provide the highest joint strength. This is because the symmetrical loading minimizes secondary bending and fastener rotation, so that loading on the bore of the fastener hole is reasonably uniform.

Single-shear joints (similar to single-lap joints) generally have lower joint strengths but are widely used in aircraft construction, for example, when access is limited to only one side during assembly. Strength loss can be minimized if the joint is well supported. However, in highly loaded applications, some degree of non-uniform loading of the bore of the fastener hole is inevitable.

Single-shear joints are often based on the use of blind fasteners. These are fasteners (described in more detail later) designed to be clamped up from one side. Alternatively, for blind fastening, bolts can be used that screw into nuts in nut plates applied to the (pre-drilled) skin before assembly. Typical applications for blind fastening are in the attachment of skins to substructure. In this type of application, countersunk or flush fasteners are often used to maintain aerodynamic smoothness.

This use of single-shear joints (even in the absence of secondary bending) and countersunk holes leads to two significant new problems: fastener rotation due to unsymmetrical loading of the joint, and reduced bearing area in the fastener hole caused by the countersink.

Considering first the use of countersinking, in the absence of fastener rotation, the bearing area is only that provided by the parallel section of the hole. This reduced bearing area could be factored into plots such as in Figures 9.30 and 9.36. Provided that clamping is sufficient and enough parallel section remains, bearing failure can be avoided, at least for lightly loaded applications. However, in many applications with thin composite skins, the countersinking may use up the entire skin thickness to accommodate the heads of available fasteners, leaving a knife-edge. Bearing strength will then be negligible, and hole elongation will occur in service unless bearing loads are very low.

Fastener rotation is a major problem in single-shear joints, resulting in marked strength reduction. It is particularly a problem with composites, even when not countersunk, because their relatively low bearing strength results in local bearing failure. Under extreme loading or due to hole elongation under cyclic loading, pull-out of the fastener or failure of the fastener head can occur, as illustrated in Figures 9.23.

With skins having countersunk holes, rotation of the faster results in the bearing surface moving onto the countersunk surface from the parallel section. However, this situation arises only once the parallel section has failed under the severe bearing pressure developed by the rotating fastener.

9.4.7 General Materials Engineering Aspects

9.4.7.1 Fasteners for Composites. Options for composite joints include either metallic or non-metallic fasteners. Flush fasteners are used for aerodynamic smoothness or to provide clearance in moving surfaces. A wide variety of fasteners is available, many specially designed for use with composites. It is beyond the scope of this chapter to describe these special fasteners in any detail; more information is provided by Niu[51] and by the relevant manufacturers' data sheets.

Metallic fasteners. To avoid galvanic corrosion problems with carbon/epoxy metallic fasteners are limited to those made of titanium alloy, stainless steel, or Inconel. Other metals, such as aluminum and low-alloy steels, may be used if they can be insulated to avoid direct contact with the composite. Generally, tension head (large head) fasteners are used to avoid problems with fastener pull-through.

Metallic fasteners are, broadly, divided into:

- Rivets—permanent fasteners clamped by:
  - plastic deformation of the shaft of the rivet
  - direct swaging of a deformable sleeve over a solid shaft
  - deformation by drawing of a sleeve over a shaped hollow shaft; these are blind fasteners. To allow development of an interference fit, some fasteners of this type include a deformable metal sleeve.
- Bolts—permanent or demountable fasteners using a nut (of a softer material) on a threaded end of the shaft clamped by:
  - standard spanners or sockets, and locked by pins or self-locking nuts
  - a tool that deforms a collar (special nut) to a design level of torque, thereby locking the collar to the shaft
  - a nut, acting on the same side as the head, that draws the collar over a hollow shaft by means of a threaded bar passing through the shaft
  - a nut, attached by a nut plate to the lower skin

Non-metallic fasteners. Non-metallic fasteners are based on reinforced thermosets or thermoplastics. As outlined by Niu,[51] non-metallic fasteners are used to:

- Avoid fuel tank arcing during lightning strike
- Reduce weight
- Increase electromagnetic transparency, reducing radar cross section
- Eliminate corrosion problems

Non-metallic fasteners do not have the load-bearing capacity of titanium or steel fasteners, but, they can rival aluminum alloy fasteners in some applications.

Fasteners made of thermoplastic matrix composites are similar to those made of metals. For example, rivets based on short-discontinuous-fiber thermoplastic composites can be formed by using an ultrasonic punch or by a conventional punch following preheating of the rivet. Similar "blind" approaches to those described for metals can also be used on preheated rivets.

9.4.7.2 Fastener Hole Preparation. Hole formation in carbon/epoxy composites using well-maintained tungsten-carbide-tipped drills poses no particular problems, provided some simple precautions are taken. Diamond-tipped drills, though more expensive, provide the best performance. Care must be taken to support the laminate during drilling by clamping it either between scrap material or in a drilling jig. The tendency for delamination on the exit side of the drill can also be reduced by coating the composite on this side with a layer of adhesive. Delamination can also be minimized by using a pressure-controlled drill at a fairly slow feed rate. Under mass-production conditions, some minor delamination damage is probably inevitable, but generally not serious, and can be repaired by resin injection, as described in the next section.

Although very good tolerances can be maintained in holes in carbon/epoxy, interference fit fastening is generally (although not universally) avoided. This is because excessive interference can lead to delamination damage during fastener installation; significant stressing of the hole can also arise in service due to the higher thermal expansion of the fastener. However, tight fit of the fastener can considerably improve fatigue performance, particularly if load reversal occurs.

For applications involving flush fasteners, countersink depths should be limited to 65% of the depth of the hole to avoid the formation of knife-edge bearing surfaces, which are very fragile in composites.

9.4.7.3 Hole-Strengthening Procedures. Several procedures involving bonded reinforcements may be used to increase the bearing load of composites. These include incorporation of extra layers into the laminate, bonding of doublers over the region of the hole, and bonding of inserts into the fastener hole.

Although composites lend themselves well to modifications to the laminate structure, manufacturing costs are significantly increased. Also, the use of bonded reinforcements may make effective repairs more difficult, or even impossible, to implement. Consequently, these approaches are limited to use in critical locations such as highly loaded lugs. Use of expanded inserts or sleeves in the fastener hole is a more cost-effective approach that also allows repairs to be undertaken relatively easily.

The stress concentration at the edges of a loaded hole in carbon/epoxy can be reduced significantly, either by local reinforcement with a stiffer fiber, such as boron, or by local softening with a low-modulus fiber such as aramid or glass. These plies are incorporated into the laminate on each side of the prospective faster hole during manufacture.

Another method of softening is the incorporation of extra $\pm 45^\circ$ carbon/epoxy plies or layers of thin titanium alloy sheet. These approaches are effective in improving both the net and bearing strength. The titanium alloy is particularly effective in increasing bearing strength. All inserts additionally reduce bearing stress by increasing the local skin thickness.

A simpler and much less costly approach is to reinforce the hole with an externally bonded doubler, made either of composite or titanium alloy.

The doubler must be appropriately scarfed to minimize shear and peel stresses in the adhesive.

In an experimental study in which the weight and extra thickness of each of these concepts were compared for a given load-carrying capacity, it was found that the extra $\pm 45^\circ$ plies provided the lightest solution and the titanium interleaves the thinnest. However, the use of titanium created considerable manufacturing difficulties because of the bonding pretreatment required and the subsequent difficulty in forming the holes.

9.4.7.4 Corrosion Prevention. Carbon/epoxy is electrically conducting and cathodic with respect to most airframe alloys other than titanium. Thus, to avoid galvanic corrosion on the metallic side of the joint, special precautions are required. In areas where carbon/epoxy and aluminum alloys may come into contact with one another, an insulating layer of glass/epoxy or aramid/epoxy is used. This is usually cocured onto the surface of the carbon/epoxy laminate during manufacture. In some cases, the insulating layer may also be used on the outside of the component to avoid electrical contact through the fasteners.

As mentioned earlier, unless insulation is possible, aluminum alloy or steel fasteners are avoided. Titanium alloy is the preferred fastener material, although stainless steel or Inconel are also suitable, but at a weight penalty. Where the titanium fasteners come into contact with the aluminum alloy side of the joint, a strontium chromate pigmented coating may be used for corrosion prevention. Corrosion-resistant steel nuts and washers, when used, will be cadmium plated if they are to come into contact with aluminum.

9.4.7.5. Component Alignment in Joints. Joints in airframe structures often require shimming in assembly to maintain correct alignment. Use of shimming is one of the most costly operations in manufacturing airframe components. Composite parts require more shimming than similar metals parts for two main reasons:

(1) Manufacturing tolerances are lower because of thickness variations associated with slight changes in composite resin content, resulting from variation in pre-preg, in resin bleed during manufacture, and in manufacturing methods.
(2) Composites are much less tolerant to force-fitting due to their high modulus and inability to yield. This will be much more of a problem with thick-section material; use of force during assembly has resulted in delamination damage in several cases.

Various approaches are possible for shimming,[51] These are:

- Solid shims, laminated titanium or stainless steel, or composite
- Laminated (peelable) shims, titanium, stainless steel, or Kapton
- Moldable, cast-in-place plastic

The moldable shim, which is the most versatile and effective for gaps up to 0.5 mm (0.020 in), involves injection of the liquid shim material into the gap between the joint components, for example, through a fastener hole. The shim material must have medium viscosity (sufficient to flow into the gap and then stay there), low shrinkage, stability in the service operating environment (temperature, moisture, fuel, etc.), and have a working life of 1 to 4 hours. Once injected into the gap, it must cure within a reasonable time at ambient temperature or around an hour at 80–90 °C.

Considerable savings are possible with composite structure if suitable manufacturing techniques can be developed to avoid the need for shimming (e.g., the co-forming of parts to ensure accurate fit irrespective of minor variation in tolerances).

9.4.8 Bonded and Bolted Joints

A joint bonded with a structural adhesive is usually much stiffer than a similar joint joined by mechanical fastening, even when the mechanical joint is optimally designed and interference fit fasteners are used. Thus it is not possible to design a joint in which the load is effectively shared between the bonded and fastened regions. Hart-Smith,[56] using his A4EK program, showed that for an optimally designed step-lap joint the bolts transmit only around one percent of the total load. However, fastening and bonding can be beneficially used together for several reasons:

- Fasteners provide an alternate in-plane load path as well as through-thickness reinforcement and therefore can contain the spread of damage in thick-section composite-bonded joints where failure (for example, due to an overload or to the development of local bond or interlaminar flaws) would occur by disbonding of the adhesive layer or by delamination of the composite.
- Fasteners can be used at the end of a lap joint, (Fig. 9.13) to reduce peel stresses. However, this is a somewhat hazardous application because the fastener holes, unless very carefully sealed, allow environmental ingress into the bond interface in the most critical region.
- Fasteners can be used both as a jigging aid and to apply pressure during adhesive bonding of composite components; generally, this approach would be effective only with paste adhesives.
- Bonding can be used to alleviate local stresses in the metallic component in a mechanically fastened joint, markedly improving fatigue and static strength properties. For the reasons mentioned, the bond line carries most of the load, and the fasteners become effective only after bond failure. This approach is extensively used with riveting in the metallic longitudinal fuselage splice region in commercial aircraft. With composite construction, this approach is more likely to be used for rework of areas found to be prone to damage.

Use of combined bolting and bonding in the repair of composite structure is considered in Chapter 10.

References

[1]Hart-Smith, L. J., *An Engineers Viewpoint on Design and Analysis of Aircraft Structural Joints*, Douglas Paper MDC 91K0067, presented at the International Conference on Aircraft Damage and Repair, Melbourne, Australia, 1991.

[2]Baker, A. A., "Joining of Advanced Fibre Composite," Chapter 8 in *Composite Materials for Aircraft Structures*, edited by B. C. Hoskin and A.A. Baker, AIAA Education Series, AIAA, New York, 1986.

[3]Hart-Smith, L. J., *Analysis and Design of Advanced Composite Bonded Joints*, NASA CR-2218, 1974.

[4]Thrall, E. W., *Failures in Adhesively Bonded Structures, Bonded Joints and Preparation for Bonding*, AGARD-CP-102, 1979.

[5]Vinson, J. R., "On the State of the Technology in Adhesively Bonded Joints in Composite Material Structures," *Emerging Technologies in Aerospace Structures Design, Structural Mechanics and Materials*, edited by J. R. Vinson, ASME, Fairfield, NJ, 1980.

[6]Mathews, F. L., Kilty, P. F., and Godwin, E. W., "A Review of the Strength of Joints in Fibre-Reinforced Plastics," *Composites*, Vol. 13, 1982, pp. 29–37.

[7]Hart-Smith, L. J., "Stress Analysis: A Continuum Mechanics Approach," in *Developments in Adhesives* 2, edited by A. J. Kinloch, Applied Science Publishers, London, 1981.

[8]Hart-Smith, L. J., *Adhesive-Bonded Double Lap Joints*, NASA CR-112235, Jan. 1973.

[9]"Guide to the Use of Data Items in the Design of Bonded Joints," Data Item 81022, Engineering Sciences Data Unit (ESDU), London, 1981.

[10]Adams, R. D., "Stress Analysis: A Finite Element Approach," *Developments in Adhesives* 2, edited by A. J. Kinloch, Applied Science Publishers, London, 1981.

[11]Hart-Smith, L. J., and Thrall, E. W, "Structural Analysis of Adhesive-Bonded Joints," *Adhesive Bonding of Aluminium Alloys*, edited by E. W. Thrall and R. W. Shannon, Marcel Dekker, New York, 1985, Chap. 13.

[12]Jones, R., "Crack Patching: Design Aspects," *Bonded Repair of Aircraft Structures*, edited by A. A., Baker and R., Jones, Martinus-Nijhoff, 1988.

[13]Chalkly, P. D., *Mathematical Modelling of Bonded Fibre: Composite Repairs to Metals*, Dept. of Defence and Technology Organisation, Aeronautical Research Laboratory, Research Report Commonwealth of Australia, AR-008–365, 1993.

[14]Hart-Smith, L. J., "Designing to Minimise Peel Stresses in Adhesive Bonded Joints," *Delamination and Debonding of Materials*, edited by W. S., Johnson, ASTM 876, 1985.

[15]Adams, R. D., and Peppiatt, N. A., "Stress Analysis of Adhesive-Bonded Lap Joints," *Journal of Strain Analysis*, Vol. 9, 1974, pp. 185–196.

[16]Crocombe, A. D., "Global Yielding As Failure Criterion for Bonded Joints," *International Journal of Adhesion*, Vol. 9, 1989, pp. 145–153.

[17]Hart-Smith, L. J., *Effects of Flaws and Porosity on Strength of Adhesive-Bonded Joints*, Douglas Paper 7388, 29th Annual SAMPE Symposium and Technical Conference, 1984.

[18]Lubin, J. L., "A Theory of Adhesive Scarf Joints," *Journal of Applied Mechanics*, Vol. 24, 1957, pp. 255–260.

[19]Kieger, R. B., "Stress Analysis Concepts for Adhesive Bonding of Aircraft Primary Structure," *Adhesively Bonded Joints: Testing, Analysis, and Design*, edited by W. S., Johnston, ASTM STP 981, 1988.

[20]Chalkley, P. D., and Chiu, W. K., "An Improved Method for Testing the Shear Stress/Strain Behaviour of Adhesives," *International Journal of Adhesion and Adhesives*, Vol. 4, 1993, pp. 237–242.

[21]Johnson W. S., and Dillard D. A., "Experimentally Determined Strength of Adhesively Bonded Joints," *Joining Fibre Reinforced Plastics*, edited by F. L. Mathews Elsevier Applied Science, 1987, pp. 105–183.

[22]Kinloch, A. J., and Shaw, S. J., "Fracture Resistance of a Toughened Epoxy Adhesive," *Journal of Adhesion*, Vol. 12, 1981, pp. 59–77.

[23]Russell, A. J., and Street, K. N., "Moisture and Temperature Effects on the Mixed Mode Delamination Fracture of Unidirectional Carbon/Epoxy," *Delamination and Disbonding of Materials*, edited by W. S., Johnson, ASTM STP 876, 1985.

[24]Loss, K. R., Ehlers, S. M., and Kedward, K. T., "An Evaluation of Cracked Lap Shear Testing for Bonded Joint Applications," *AIAA/ASME/ASCE/AAS Collection of Technical Papers*, New York, 1985, pp. 647–655.

[25]Hart-Smith, L. J., "Difference Between Adhesive Behaviour in Test Coupons and Structural Joints," Douglas Paper 7066, presented to ASTM Adhesives Committee, Phoenix, AZ, 1986.

[26]Russell, A. J., "Fatigue Crack Growth in Adhesively Bonded Carbon/Epoxy Joints Under Shear Loading," *ASME Symposium on Advances in Adhesively Bonded Joints*, edited by S. Mall, K. M. Liechti, and J. K. Vinson, Vol. 6, Book No GOO485, 1988.

[27]Lin, C., and Liechti, K. M., "Similarity Concepts in the Fatigue Fracture of Adhesively Bonded Joints," *Journal of Adhesion*, Vol. 21, 1987, pp. 1–24.

[28]Mall, S., and Yun, K. T., "Effect of Cyclic Ductility on Cyclic Debond Mechanism in Composite-to-Composite Bonded Joints," *Journal of Adhesion*, Vol. 23, 1987, pp. 215–231.

[29]Baker, A., "Crack Patching: Experimental Studies, Practical Applications," *Bonded Repair of Aircraft Structures*, edited by A. A. Baker and R. Jones, Martinus-Nijhoff, 1988.

[30]Johnson W. S., and Mall, S., *Influence of Interface Ply Orientation on Fatigue Damage of Adhesively Bonded Composite Joints*, ASTM Composite Technology Review, 1986.

[31]Comyn, J., "The Relationship Between Joint Durability and Water Diffusion," *Developments in Adhesives*, edited by A. J. Kinloch, Applied Science Publishers, London, 1981, Chap. 2.

[32]Crank, J., *Mathematics of Diffusion*, Oxford Univ. Press, 1956.

[33]Kinloch, A. J., "The Service Life of Adhesive Joints," *Adhesion and Adhesives: Science and Technology*, Chapman Hall, 1987, Chap. 8.

[34]Chester, R. J., and Baker, A. A., *Environmental Durability of Carbon/epoxy F/A-18 Composites, Proceedings of ICCM-10* 1995.

[35]Hart-Smith, L. J., Ochsner, R. W., and Radecky, R. L., *Surface Preparation of Fibrous Composites for Adhesive Bonding or Painting*, First Quarter Issue Douglas Service, 1984.

[36]Hart-Smith, L. J., Wong, S. B., and Brown, D. L., *Surface Preparations for Ensuring That the Glue Will Stick in Bonded Composite Structures*, NAWCADWAR-94096-60, 1994, (also McDonnell Douglas Paper 93K0126, 1993).

[37]Parker, B. M., and Waghorne, R. M., "Surface Pretreatment of Carbon Fibre Reinforced Composites for Adhesive Bonding," *Composites*, Vol. 13, 1982, pp. 280–288.

[38]Poncuis, A. V., and Wenz, R. P., "Mechanical Surface Preparation of Carbon-Epoxy Composites for Adhesive Bonding," *SAMPE Journal*, Vol. 21, 1985, pp. 50–57.

[39]Kinloch, A. J., and Taig, C. M., "The Adhesive Bonding of Thermoplastic Composites," *Journal of Adhesion*, Vol. 29, 1987, pp. 291–302.

[40]Kodokian, G. K. A., and Kinloch, A. J., "The Adhesive Fracture Energy of Bonded Thermoplastic Fibre-Composites," *Journal of Adhesion*, Vol. 29, 1989, pp. 193–218.

[41]Davies, P., Cantwell, W. J., Jar, P. Y., Bourban, P. E., Zyman, V., and Kauch, H. H., "Joining and Repair of Fibre-Reinforced Thermoplastic," *Composites*, Vol. 22, 1991, pp. 425–431.

[42]Hart-Smith, L. J., "Mechanically-Fastened Joints for Advanced Composites" *Fibrous Composites in Structural Design*, edited by E. M. Lenoe, D. W. Oplinger, and J. J. Burke, Plenum Press, New York, 1980.

[43]Leknitski, S. G., *Anisotropic Plates*, 2nd ed., Gordon and Breach, New York, 1968, pp. 171.

[44]Davis, M. J., and Jones, R., *Damage Tolerance of Fibre Composite Laminates in Composite Materials for Aircraft Structures*, edited by B. C. Hoskin and A. A. Baker, AIAA Education Series, AIAA, New York, 1986 Chap. 10.

[45]Soni, S. R., *Failure Analysis of Composite Laminates with a Fastener Hole*, edited by K. T., Kedward, ASTM STP 749, American Society for Testing Materials, 1981, pp. 145–164.

[46]Chang, F. K., Scott, R. A., and Springer, G. S., "Failure of Composite Laminates Containing Pin Loaded Holes: Method of Solution," *Journal of Composite Materials*, Vol. 18, 1984.

[47]Bailie, J. A., Duggan, M. F., Bradshaw, N. C., and McKenzie, T. G., "Design Data for Carbon Cloth Epoxy Bolted Joints at Temperatures up to 450 K," *Joining of Composite Materials*, edited by K. T. Kedward, ASTM STP 749, American Society for Testing and Materials, 1981, pp. 165–180.

[48]Wu, P. S., and Sun, C. T., "Modelling Bearing Failure Initiation in Pin-contact of Composite Laminates," *Mechanics of Materials*, Vol. 29, 1998, pp. 325–335.

[49]Collins, T. A., "The Strength of Bolted Joints in Multidirectional CFRP Laminates," *Composites*, Vol. 8, 1977, pp. 43–55.

[50]Crews J. H., Jr. "Bolt-Bearing Fatigue of a Carbon/Epoxy Laminate," *Joining of Composite Materials*, edited by K. T. Kedward, ASTM STP 749, American Society for Testing and Materials, 1981, pp. 131–144.

[51]Niu, M. C. Y., "Joining" *Composite Airframe Structures*, Conmilit Press, Hong Kong, 1992, Chap. 5.

[52]Crews, J. H., and Naik, R. A., "Combined Bearing and Bypass Loading on a Carbon/Epoxy Laminate," *Composite Structures*, Vol. 6, 1986, pp. 21–40.

[53]Nelson, W. D., Bunin, B. L., and Hart-Smith, L. J., *Critical Joints in Large Composite Structure*, Douglas Paper 7266, presented at Sixth Conference on Fibrous Composites in Structural Design, 1983.

[54]*Fatigue of Filamentary Composites*, ASTM STP 636, 1977.

[55]Saunders, D. S., Galea, S. C., Deirmendjian, G. K., "The Development of Fatigue Damage Around Fastener Holes in Thick Carbon/Epoxy Composite Laminates," *Composites*, Vol. 24, 1993, pp. 309–321.

[56]Hart-Smith, L. J., "Design Methodology for Bonded-Bolted Composite Joints," Vol. 1, *Analysis Derivations and Illustrative Solutions*, AFWAL-TR-81–3154.

[57]"Flexibility of, and bad distribution in, multi-bolt lap joints subject to in-plane axial loads," Data Item 98012, Engineering Sciences Data Unit (ESDU), London, 2001.